



An effective quantum artificial rabbits optimizer for energy management in microgrid considering demand response

Nehmedo Alamir^{1,2} · Salah Kamel² · Mohamed H. Hassan^{2,3} · Sobhy M. Abdelkader^{1,4}

Accepted: 11 June 2023 / Published online: 10 July 2023
© The Author(s) 2023

Abstract

Solving the energy management (EM) problem in microgrids with the incorporation of demand response programs helps in achieving technical and economic advantages and enhancing the load curve characteristics. The EM problem, with its large number of constraints, is considered as a nonlinear optimization problem. Artificial rabbits optimization has an exceptional performance, however there is no single algorithm can solve all engineering problem. So, this paper proposes a modified version of artificial rabbits optimization algorithm, called QARO, by quantum mechanics based on Monte Carlo method to determine the optimal scheduling for MG resources effectively. The main objective is minimization of the daily operating cost with the maximization of MG operator (MGO) benefit. The operating cost includes the conventional diesel generator operating cost and the cost of power transactions with the grid. The performance of the proposed algorithm is assessed using different standard benchmark test functions. A ranking order for the test function based on the average value and Tied rank technique, Wilcoxon's rank test based on median value, and Anova Kruskal–Wallis test showed that QARO achieved best results on the most functions and outperforms all other compared technique. The obtained results of the proposed QARO are compared with those obtained by employing well-known and newly-developed algorithms. Moreover, the proposed QARO is used to solve two case studies of day-ahead EM problem in MG, then the obtained results are also compared with other well-known optimization techniques, the results demonstrate the effectiveness of QARO in reducing the operating cost and maximization the MGO benefit.

Keywords Quantum mechanism · Optimization · Energy management · Demand response · Artificial rabbits optimization · Microgrid

1 Introduction

Microgrids (MGs) are small-scale networks, which consist of renewable energy sources (RES), conventional generation sources, energy storage systems (ESS), and controllable/non-controllable loads (Lasseter and Microgrids 2002; Shivam and Dahiya 2018). The flexible operation of MGs resources enables the possibility of using various optimization techniques to achieve technical, environmental and economic benefits (Phani Raghav et al. 2022). Energy management systems (EMS) are required for MGs to achieve objectives, such as minimization of operating costs, reduced losses, and improved reliability. These objectives depend on the efficient management of resources, flexible loads, and energy transactions with the grid (Parisio et al. 2014). MG's energy management (EM)

✉ Nehmedo Alamir
Nehmedo.Alamir@ejust.edu.eg

Salah Kamel
skamel@aswu.edu.eg

Mohamed H. Hassan
mohamedhosnymoe@gmail.com

Sobhy M. Abdelkader
sobhy.abdelkader@ejust.edu.eg

¹ Electrical Power Engineering, Egypt-Japan University of Science and Technology, New Borg El-Arab City, Egypt

² Department of Electrical Engineering, Faculty of Engineering, Aswan University, Aswan 81542, Egypt

³ Ministry of Electricity and Renewable Energy, Cairo, Egypt

⁴ Department of Electrical Engineering, Faculty of Engineering, Mansura University, Elmansoura, Egypt

recently received great attention for MG's resources optimal operation.

Different structures have been proposed for EMS utilizing a variety of optimization algorithms and energy sources. To reduce the operating cost in MG, a multi-objective genetic algorithm (MOGA) is employed in Torkan et al. (2022). Ref. Aguila-Leon et al. (2022), a Particle swarm optimization (PSO) algorithm is employed to incorporate the RESs to the EMS of the MG efficiently. A developed manta ray foraging optimization (DMRFO) in Dong et al. (2022) is used to reduce the operating cost and emissions in the MG. For MG capacity planning, Ref. Bukar et al. (2022) employed seven different optimization algorithms: grey wolf optimization (GWO), dragonfly algorithm (DFA), cuckoo search algorithm (CSA), the grasshopper optimization algorithm (GOA), Salp swarm algorithm (SSA), ant lion optimization (ALO), and PSO.

By integrating intelligent technologies in MGs, communication may be created between MG consumers and the EMS, as well as between the EMS and the main grid. Thus, Demand response programs (DRP) can contribute significantly to cost savings (Rahimiyan et al. 2014). Also, the use of DRP can enhance the load curve by allowing the positive contribution of the customers (Palensky and Dietrich 2011). DR is defined as changing customers' power consumption in response to fluctuating electricity prices or incentive payments (Aalami et al. 2010). There are two different categories of DR: Incentive-based DR (IDR) and price-based DR (Jordehi 2019). Numerous studies have been conducted on the efficient implementation of DR into and its contribution to the demand–supply balance, grid reliability, and performance, particularly in MG with its distributed generation (DG) sources. Robert et al. (2018) and Parisio et al. (2014) examined the effectiveness of integrating DR with MG in order to achieve environmental and economic benefits. In Shehzad Hassan et al. (2019) PDR is incorporated in the EMS of the MG, using PSO the MG's profit is maximized for different pricing strategies. In Faria et al. (2013), to reduce the MG's operating cost PSO algorithm was employed in EMS for achieving optimal scheduling to the DR and MG. A genetic algorithm (GA) is used in Wang et al. (2018) for optimal scheduling of MG's resources with a PDR program. Also, GA is embedded in the EMS of MG for reduction of the operating cost in Arif et al. (2014). A combination of modified PSO and differential Evolutionary (DE) algorithm with IDR is used to solve the problem of EM and planning in Sedighzadeh et al. (2019). In Soroudi et al. (2016), a PDR is developed for the minimization of power losses in MG. Based on real-time pricing, Ref. presented Yu and Hong (2016) a DR for the optimal EM. Different DRP

types are employed in the EMS of Multi-Microgrid the problem is solved using linear programming with mixed integer linear programming (MILP) mathematical models in Nguyen et al. (2018). To reduce the operating cost and to maximize the operator benefit is the EM problem solved using Honey Badger Optimizer (HBA) in Alamir et al. (2022b) and using Alamir et al. (2022a) Artificial Hummingbird Algorithm (AHA).

According to the aforementioned studies, various optimization techniques have been employed to solve different engineering problems effectively, particularly for different EMS objectives. So these researches revealed a chance for establishing new and improved optimization strategies for solving specific problems. Also, thanks to the No-Free-Lunch (NFL) theorem (Wolpert and Macready 1997), which state that “there are no metaheuristic optimization algorithms capable of addressing all optimization problems and guarantee the same performance”. These two previously mentioned reasons clarify our motivation to propose the Quantum Artificial Rabbits Optimization (QARO) as an improved version of Artificial rabbits optimization (Wang et al. 2022) which was chosen owing to their exceptional performance in solving a variety of mathematical and engineering design problems. A summary comparison for the related work is shown in Table 1.

The objective of this paper is to introduce a QARO algorithm based on the quantum mechanics to enhance the conventional ARO. The second objective is to optimize the MG operation taking incentive DR into account and comparing to other optimization metaheuristics.

The following are the principal contributions of this work to the investigation, as mentioned earlier:

1. A Quantum Artificial Rabbits Optimization is proposed to enhance the performance of the original ARO algorithm and to solve the EM problem in MG. A quantum mechanics by employing the Monte Carlo method is used to prevent premature convergence to local minimum.
2. Considering the demand response program, the EM problem in MG is solved by employing the proposed QARO algorithm. And its performance is compared with well-known and newly developed algorithms to solve the EM problem.

The rest of this paper is structured as follows: Sect. 2 presents the modeling of the Grid-connected Microgrid with modeling of DRP. Section 3 discusses the EM optimization problem modeling; Sect. 4 focuses on the traditional ARO and the proposed QARO algorithms. The obtained simulation results are presented in Sect. 5. Finally, the paper is concluded in Sect. 6.

Table 1 Summary for the related work

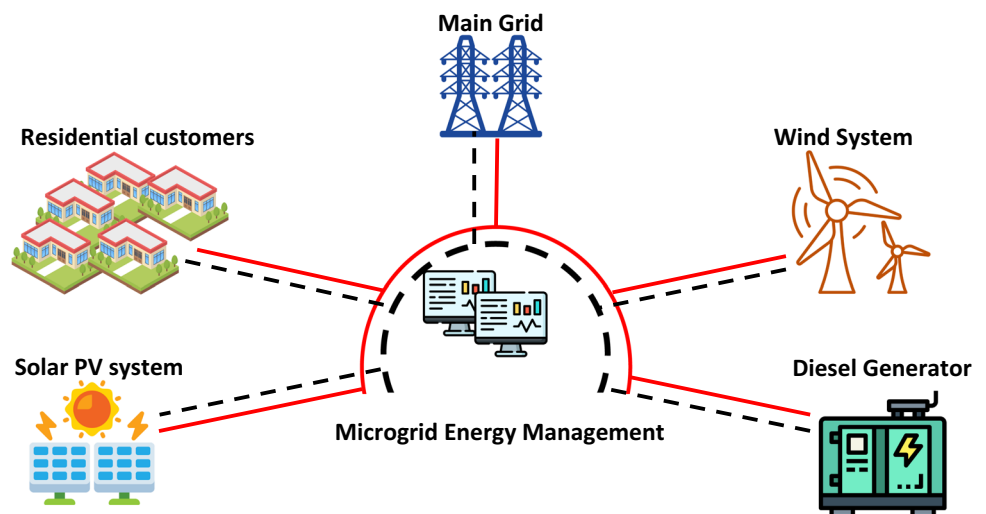
Refs.	Formulation	Objectives	Proposed optimization technique	DR	MG benefit
Faria et al. (2013)	Single-objective PSO	Operating cost minimization	✗	✓	✗
Arif et al. (2014), Wang et al. (2018)	Single-objective GA	Operating cost minimization	✗	✓	✗
Soroudi et al. (2016)	Robust Optimization technique	Single-objective Power losses minimization	✗	✓	✗
Yu and Hong (2016)	A one-leader, N-follower Stackelberg game	Minimize the load during high energy prices	✓	✓	✗
Nguyen et al. (2018)	MILP	Operating cost minimization	✗	✓	✗
Shehzad Hassan et al. (2019)	Single-objective PSO	Profit maximization for customers	✗	✓	✗
Sedighzadeh et al. (2019)	PSO and differential Evolutionary	Multi-objective Cost and emissions minimization	✗	✓	✗
Torkan et al. (2022)	Multi-objective (GA) MOGA	Operating cost minimization Emissions minimization	✗	✓	✗
Dong et al. (2022)	Multi-objective DMRFO	Operating cost minimization Emissions minimization		✗	–
Bukar et al. (2022)	Single-objective GWO, DFA, CSA, GOA, SSA, ALO, and PSO	MG capacity planning based on net-present cost minimization	✗	✗	–
Alamir et al. (2022a, b)	Multi-objective HBA and AHA	Cost minimization Benefit maximization	✗	✓	✓
This paper	Multi-objective QARO	Cost minimization Benefit maximization	✓	✓	✓

2 Problem formulation

The proposed grid-connected MG scheme is shown in Fig. 1, which consists of Dispatchable conventional sources such as conventional diesel generator (CDG), renewable sources such as Photovoltaic (PV), Wind Turbine

(WT), and responsive residential customers (RC) as described below. The MG is assumed to have a connection to the Utility Grid (UG) with the possibility of two way energy transactions.

Fig. 1 The overall scheme of the grid-connected MG



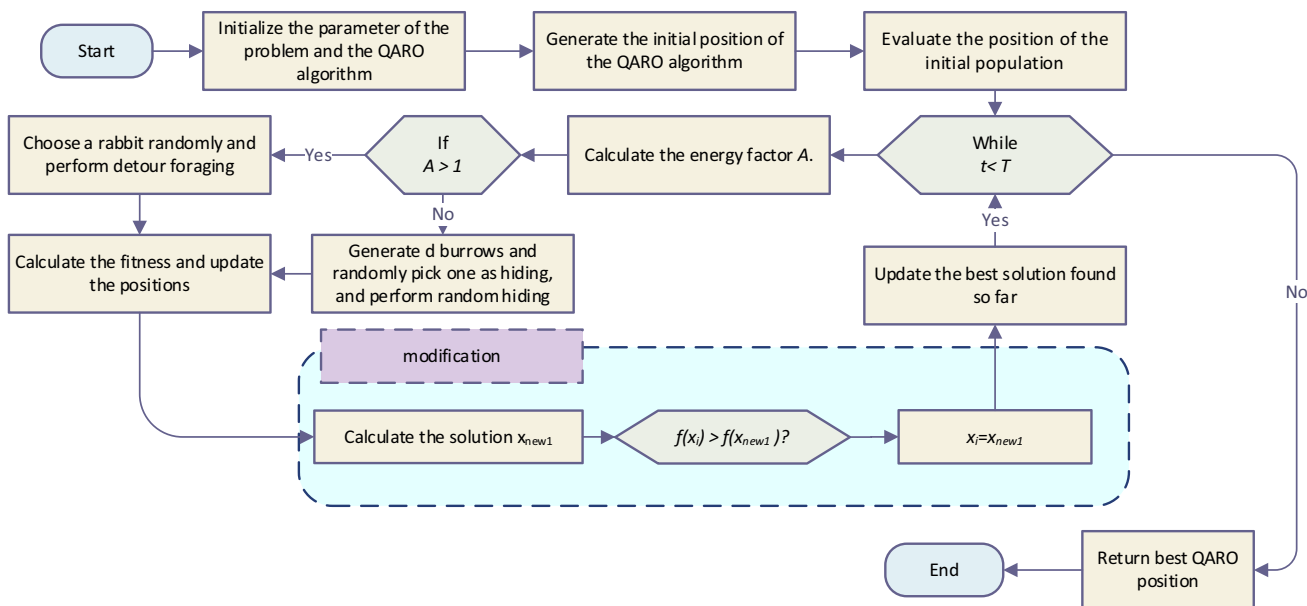


Fig. 2 Flowchart of QARO algorithm

2.1 Utility grid power transaction

If we denote the amount of power transaction with the UG at any time interval t as $P_{UG,t}$, then the Locational Marginal Prices (LMP’s) (γ_t) (Nwulu and Fahrioglu 2013) is employed to express the cost of power transaction $C_{UG}(P_{UG,t})$ as:

$$C_{UG}(P_{UG,t}) = \gamma_t \times P_{UG,t} \tag{1}$$

2.2 Generation model

a. WT model

WT output power is Probabilistic in its nature; the generated power ($P_{wind,t}$) is entirely dependent on wind speed ($v_{hub,t}$) at the hub height h_{hub} , Wind speed can be calculated based on the reference wind speed ($v_{ref,t}$) at the reference height h_{ref} as Tazvinga et al. (2014):

$$v_{hub,t} = v_{ref,t} \left(\frac{h_{hub}}{h_{ref}} \right)^\beta \tag{2}$$

where β is the power law exponent in the range of $\frac{1}{7}$.

The WT hourly generated power is given as:

$$P_{wind,t} = 0.5n_w p_{air} C_p A v_{hub,t} \tag{3}$$

where A is the swept area by the rotor; n_w is the efficiency of WT; p_{air} air density; C_p is the power coefficient of the turbine.

b. Solar PV model

The hourly generated power from PV solar array depends on the incident solar irradiation on the PV array $I_{PV,t}$ (kW h/m²) and it is expressed as Tazvinga et al. (2013):

$$P_{PV,t} = \eta_{PV} A_c I_{PV,t} \tag{4}$$

Also, solar power depends on the efficiency of the solar array (η_{PV}), and the PV array area A_c (Tazvinga et al. 2013).

c. CDG and load model

The CDG is considered as an essential generation source in MGs. The output power of these CDGs can be adjusted flexibly by the operator. The fuel cost of CDG $C_i(P_{CDG,i,t})$ can be expressed by the quadratic model as:

$$C_i(P_{CDG,i,t}) = a_i P_{CDG,i,t}^2 + b_i P_{CDG,i,t} \tag{5}$$

where i is the CDG number; a_i and b_i are fuel cost coefficients.

Usually, load is modelled by adding up the separate customer loads. In this paper, customers are grouped according to their participation in DRP.

2.3 Demand response model

If the customer type is θ , which refers to its willingness to participate in the DR program and $P_{c,j,t}$ is the amount of consumption reduction; then customer’s j cost function ($C_j(\theta, P_{c,j,t})$) can be expressed as Fahrioglu and Alvarado (2000):

$$C_j(\theta, P_{c_{j,t}}) = k_1 P_{c_{j,t}}^2 + k_2 P_{c_{j,t}}(1 - \theta) \tag{6}$$

where k_1 , and k_2 are cost coefficients,

Then the benefit of the responsive customer is calculated as:

$$B_{1,j}(\theta, y, P_{c_{j,t}} = y_{j,t} - (k_1 P_{c_{j,t}}^2 + k_2 P_{c_{j,t}} - k_2 P_{c_{j,t}}), \tag{7}$$

for $j = 1, 2, \dots, J$

where $y_{j,t}$ is the incentive payment that customer j receive. Customers will participate in DR only in case that $B_j \geq 0$.

The benefit of MG from the participation of customer j in DR program can be expressed as:

$$B_{2,j}(\theta, \lambda, P_{c_{j,t}}) = \lambda_{j,t} P_{c_{j,t}} - y_{j,t} \tag{8}$$

where $\lambda_{j,t}$ is the cost of power interruption of customer j ; its value can be calculated based on the optimal power flow analysis (Fahrioglu and Alvarado 2000).

So that the total benefit of MG is calculated based on (8) for the entire interval T as:

$$B_2 = \sum_{j=1}^J \sum_{t=1}^T \lambda_{j,t} P_{c_{j,t}} - y_{j,t} \tag{9}$$

3 Energy management problem formulation

As mentioned previously, MG’s proposed architecture in this paper consists of different types of generation sources, as WT, PV, and CDG, and responsive customers with DRP. Main objective of the EMS is to optimize the operation of these generation sources. For this purpose of solving Multi-objective optimization problems;

Following is a mathematical description of two objective functions.

Table 2 Parameter settings of the selected techniques

Algorithms	Parameters setting
Common settings	Population size: $nPop = 50$ Maximum iterations: $Max_iter = 200$ Number of independent runs: 20
GWO	θ ($= 2$ to 0)
EO	No such parameter
SDO	
ARO	
QARO	$u = [0, 1], h = [0, 1]$

3.1 Objective function

The EM problem in this paper is formulated as a multi-objective problem as following:

- (a) Minimization of the operating cost ($f_1(x)$), which is the cost of power generation and the cost of power transaction with the utility grid.

This mathematical representation of this objective function can be described as follows:

$$\min f_1(x) = \min \sum_{t=1}^T \sum_{i=1}^I C_i(P_{CDG_{i,t}}) + \sum_{t=1}^T C_{UG}(P_{UG_t}) \tag{10}$$

where I is the total number of CDG.

The first term of Eq. (10) is for CDG generation cost minimization, while the second is for the power transaction cost.

- (b) Maximization of the MG operator benefit $f_2(x)$ considering the DRP in EMS. This objective function can be expressed as:

$$\max f_2(x) = \max \sum_{j=1}^J \sum_{t=1}^T \lambda_{j,t} P_{c_{j,t}} - y_{j,t} \tag{11}$$

Therefore, the mathematical model of the objective function for MG management is represented as:

$$\min w_1 \left[\sum_{t=1}^T \sum_{i=1}^I C_i(P_{CDG_{i,t}}) + \sum_{t=1}^T C_{UG}(P_{UG_t}) \right] + w_2 \left[\sum_{j=1}^J \sum_{t=1}^T y_{j,t} - \lambda_{j,t} P_{c_{j,t}} \right] \tag{12}$$

With the following Equation should be satisfied:

$$w_1 + w_2 = 1 \tag{13}$$

where w_1 and w_2 are the weighting factors for the first and second objective functions, respectively.

3.2 Constraints

The proposed operation of the EMS operation problem is subjected to the following constraints:

3.2.1 Electrical load balance

For any time interval t the electrical load demand with DRP should equal the summation of the total generated power from PV, WT, CDGs and the power transacted with

Table 3 Benchmark functions

Name	Function	Dim	Range	f_{\min}
<i>Unimodal test functions</i>				
Sphere	$F_1(x) = \sum_{i=1}^N x_i^2$	30	[- 100,100]	0
Schwefel 2.22	$F_2(x) = \sum_{i=1}^N x_i + \prod_{i=1}^N x_i $	30	[- 10,10]	0
Schwefel 1.2	$F_3(x) = \sum_{i=1}^N \left(\sum_{j=1}^i x_j \right)^2$	30	[- 100,100]	0
Schwefel 2.21	$F_4(x) = \max_i \{ x_i , 1 \leq i \leq N\}$	30	[- 100,100]	0
Rosenbrock	$F_5(x) = \sum_{i=1}^{N-1} [100(x_{i+1} - x_i^2)^2 + (x_i - 1)^2]$	30	[- 30,30]	0
Step	$F_6(x) = \sum_{i=1}^N (x_i + 0.5)^2$	30	[- 100,100]	0
Quartic	$F_7(x) = \sum_{i=1}^N ix_i^4 + \text{random}[0, 1]$	30	[- 1.28,1.28]	0
<i>Multimodal test functions</i>				
Schwefel	$F_8(x) = \sum_{i=1}^N \sum_{j=1}^i -x_j \sin(\sqrt{ x_i })$	30	[- 500,500]	- 418.9829 × dim
Rastrigin	$F_9(x) = \sum_{i=1}^N [x_i^2 - 10 \cos(2\pi x_i)] + 10$	30	[- 5.12,5.12]	0
Ackley	$F_{10}(x) = -20 \exp\left(-0.2 \sqrt{\frac{1}{N} \sum_{i=1}^N x_i^2}\right) - \exp\left(\frac{1}{N} \sum_{i=1}^N \cos(2\pi x_i)\right) + 20 + e$	30	[- 32,32]	0
Griewank	$F_{11}(x) = \frac{1}{4000} \sum_{i=1}^N x_i^2 - \prod_{i=1}^N \cos\left(\frac{x_i}{\sqrt{ i }}\right) + 1$	30	[- 600,600]	0
Penalized	$F_{12}(x) = \frac{\pi}{n} \left\{ 10 \sin(\pi y_1) + \sum_{i=1}^{n-1} (y_i - 1)^2 [1 + 10 \sin^2(\pi y_{i+1})] + (y_n - 1)^2 \right\} + \sum_{i=1}^n u(x_i, 10, 100, 4)$	30	[- 50,50]	0
Penalized2	$F_{13}(x) = 0.1 \left\{ \sin^2(3\pi x_1) + \sum_{i=1}^n (x_i - 1)^2 [1 + \sin^2(\pi x_i + 1)] \right\} + (x_n - 1)^2 [1 + \sin^2(2\pi x_n)] + \sum_{i=1}^n u(x_i, 5, 100, 4)$	30	[- 50,50]	0
<i>Low-dimensional multimodal test functions</i>				
Foxholes	$F_{14}(x) = \left(\frac{1}{500} + \sum_{j=1}^{25} \frac{1}{j + \sum_{i=1}^j (x_i - a_{ij})^6} \right)^{-1}$	2	[- 65,65]	1
Kowalik	$F_{15}(x) = \sum_{i=1}^{11} \left[a_i - \frac{x_i (b_i^2 + b_i x_2)}{b_i^2 + b_i x_3 + x_4} \right]^2$	4	[- 5,5]	0.00030
Six Hump camel	$F_{16}(x) = 4x_1^2 - 2.1x_1^4 + \frac{1}{3}x_1^6 + x_1x_2 - 4x_2^2 + 4x_2^4$	2	[- 5,5]	- 1.0316
Branin	$F_{17}(x) = (x_2 - \frac{5.1}{4\pi^2}x_1^2 + \frac{5}{\pi}x_1 - 6) + 10(1 - \frac{1}{8\pi})\cos x_1 + 10$	2	[- 5,5]	0.398
Goldstein-Price	$F_{18}(x) = \left[1 + (x_1 + x_2 + 1)^2 (19 - 14x_1 + 3x_1^2 - 14x_2 + 6x_1x_2 + 3x_2^2) \right] \times \left[30 + (2x_1 - 3x_2)^2 \times (18 - 32x_1 + 12x_1^2 + 48x_2 - 36x_1x_2 + 27x_2^2) \right]$	2	[- 2,2]	3
Hartman 3	$F_{19}(x) = -\sum_{i=1}^4 c_i \exp\left(-\sum_{j=1}^3 a_{ij}(x_j - p_{ij})^2\right)$	3	[1,3]	- 3.86

$$y_i = 1 + \frac{x_i+1}{4} u(x_i, a, k, m) = \begin{cases} k(x_i - a)^m, & x_i > a \\ 0 - a < x_i < a \\ k(-x_i - a)^m, & x_i < -a \end{cases}$$

Table 3 (continued)

Name	Function	Dim	Range	f_{min}
Hartman 6	$F_{20}(x) = -\sum_{i=1}^4 c_i \exp\left(-\sum_{j=1}^6 a_{ij}(x_j - p_{ij})^2\right)$	6	[0, 1]	- 3.32
Shekel 5	$F_{21}(x) = -\sum_{i=1}^5 [(X - a_i)(X - a_i)^T + c_i]^{-1}$	4	[0, 10]	- 10.1532
Shekel 7	$F_{22}(x) = -\sum_{i=1}^7 [(X - a_i)(X - a_i)^T + c_i]^{-1}$	4	[0, 10]	- 10.4028
Shekel 10	$F_{23}(x) = -\sum_{i=1}^{10} [(X - a_i)(X - a_i)^T + c_i]^{-1}$	4	[0, 10]	- 10.5363

the utility grid P_{UG_t} . Thus, the electrical load balance can be modelled as:

$$\sum_{i=1}^I P_{CDG_{i,t}} + P_{wind_t} + P_{PV_t} + P_{UG_t} = P_{D,t} - \sum_{j=1}^J P_{c_{j,t}} \tag{14}$$

3.2.2 Dispatchable CDGs constraints

The output power from each CDG should be within its minimum ($P_{CDG_{i,min}}$) and maximum ($P_{CDG_{i,max}}$) limits as it is indicated in Eq. (15). Also constraint in (16) states that the ramping up and down rate (DR_i) limits should not be violated.

$$P_{CDG_{i,min}} \leq P_{CDG_{i,t}} \leq P_{CDG_{i,max}} \tag{15}$$

$$-DR_i \leq P_{CDG_{i,t+1}} - P_{CDG_{i,t}} \leq UR_i \tag{16}$$

3.2.3 Grid constraint

Power transaction with the utility constraints is as in Eq. (17), which limits the power transaction below the maximum limit ($-P_{UG_{max}}$).

$$-P_{UG_{max}} \leq P_{UG_t} \leq P_{UG_{max}} \tag{17}$$

3.2.4 Demand response constraints

Based on (7), the function of benefit for responsive customer is prolonged for the entire time horizon (1 day). This ensures that the customer incentive during the day is greater than what should be paid if electricity is consumed rather than curtailed; this limitation is expressed as:

$$\sum_{t=1}^T y_{j,t} - (k_1 P_{c_{j,t}}^2 + k_2 P_{c_{j,t}} - k_2 P_{c_{j,t}} \theta_j) \geq 0 \tag{18}$$

Constraint (19) specifies the permitted amount of customer j power curtailment, where P_{CM_j} is the customer's daily power curtailment limit.

$$\sum_{t=1}^T P_{c_{j,t}} \leq P_{CM_j} \tag{19}$$

The DRP is employed with consideration of the daily budget limit (DBL) of the MG as in the following Equation:

$$\sum_{t=1}^T \sum_{j=1}^J y_{j,t} \leq DBL \tag{20}$$

4 Solution method

4.1 Original artificial rabbits optimization (ARO)

The original ARO mimics the foraging and hiding tactics of actual rabbits, as well as their energy shrink leading to transiting between these tactics (Wang et al. 2022).

(a) Detour foraging (exploration)

In detour foraging behavior of ARO, each individual in the search space tends to update its location towards the other search individual chosen randomly from the group and add a perturbation. The following equation describe the mathematical model of the detour foraging:

$$v_i(t + 1) = x_j(t) + R \times (x_i(t) - x_j(t)) + \text{round}(0.5 \times (0.05 + r_1)) \times n_1, i, j = 1, \dots, j \neq i \tag{21.1}$$

$$R = L \times c \tag{21.2}$$

$$L = (e - e^{\frac{t-1}{T}}) \times \sin(2\pi r_2) \tag{21.3}$$

$$c(k) = \begin{cases} 1 & \text{if } k == g(l) \\ 0 & \text{else} \end{cases} \quad k = 1, \dots, d \text{ and } l = 1, \dots, [r_3, d] \tag{21.4}$$

$$g = \text{randperm}(d), n_1 \sim N(0, 1) \tag{21.5}$$

(b) Random hiding (exploitation)

To escape from predators, a rabbit commonly digs some holes nearby its nest for hiding. This equation is given in this regard as:

$$b_{i,j}(t) = x_i(t) + H.g.x_i(t), i = 1, \dots, n \text{ and } j = 1, \dots, d \tag{22.1}$$

$$H = \frac{T - t + 1}{T}.r_4, n_2 \sim N(0, 1) \tag{22.2}$$

$$g(k) = \begin{cases} 1 & \text{if } k == j \\ 0 & \text{else} \end{cases} \quad k = 1, \dots, d \tag{22.3}$$

The rabbits to be survive need to find a safe residence to hide. So, they select randomly a hole from their holes for hiding to escape from getting caught. This random hiding tactic is modeled as below:

$$v_i(t + 1) = x_i(t) + R \times (r_4 \times b_{ir}(t) - x_i(t)) i = 1, \dots, n \tag{23.1}$$

$$g(k) = \begin{cases} 1 & \text{if } k == [r_5 \times d] \\ 0 & \text{else} \end{cases} \quad k = 1, \dots, d \tag{23.2}$$

$$b_{i,r}(t) = x_i(t) + H.g.x_i(t) \tag{23.3}$$

After detour foraging or p random hiding is reached, the position update of the i th rabbit is:

$$x_i(t + 1) = \begin{cases} x_i(t) & \text{if } f(x_i(t)) \leq f(v_i(t + 1)) \\ v_i(t + 1) & \text{if } f(x_i(t)) > f(v_i(t + 1)) \end{cases} \tag{24}$$

(c) Energy shrink (switch from exploration to exploitation)

An energy factor is considered to model the switch from exploration to exploitation phases. The energy factor in this algorithm can be given as follows:

$$A(t) = 4 \left(1 - \frac{t}{T} \right) \tag{25}$$

4.2 Proposed QARO

Quantum mechanics are employed to enhance the conventional ARO technique. This quantum model of an ARO algorithm will be referred to as a QARO algorithm. The quantum mechanics was used to develop the PSO algorithm in Coelho (2008). In the quantum model, using Monte Carlo method, the solution x_{new1} can be calculated as follows Elkasem et al. (2022):

If $h \geq 0.5$

$$x_{new1} = p + \alpha \cdot |\text{Mbest}_i - X_i| \cdot \ln(1/u) \tag{26}$$

Else

$$x_{new1} = p - \alpha \cdot |\text{Mbest}_i - X_i| \cdot \ln(1/u) \tag{27}$$

End
 where α is a design parameter, u and h are uniform probability distribution in the range of $[0, 1]$, Mbest represents the mean best of the population, and it is defined as the mean of the global best positions. It is can be calculated as follows El-Sattar et al. (2022):

$$\text{Mbest} = \frac{1}{N} \sum_{l=1}^N p_{g,l}(i) \tag{28}$$

where g is the index of the best solution. The flowchart of the proposed QARO algorithm is presented in Fig. 2. Moreover, Algorithm 1 describes the QARO algorithm’s pseudocode.

Algorithm 1: Pseudocode of the QARO algorithm

Set the control parameter (Dimension of problem (d), maximum iteration, population size), and h

Initialize the population randomly

Evaluate the fitness of the new solution

Obtain the best solution

While $t \leq T$

 Calculate the energy factor A

If $A > 0.5$

 Choose a rabbit randomly and perform detour foraging

Else If $A \leq 0.5$

 Generate burrows and randomly pick one as hiding and perform random hiding

End If

 Check the limits of the new locations and evaluate the fitness values

 %Quantum mechanics

If $h > 0.5$

 Update the new location of the rabbit using Eq. (26)

Else If $h \leq 0.5$

 Update the new location of the rabbit using Eq. (27)

End If

 Check the limits of the new locations and evaluate the fitness values

 Find the new solution if the fitness is better

$t = t + 1$

End while

Output the best solution

4.3 Computational complexity analysis of QARO

Computational complexity provides a valuable tool for assessing the effectiveness of algorithms in solving optimization problems. The complexity of an algorithm is influenced by several factors, including the number of individuals involved (n), the dimensionality of the problem's variables (d), and the maximum number of iterations (T). In the case of QARO, the total computational complexity can be expressed as follows:

$$\begin{aligned}
 O(\text{QARO}) &= O(\text{problem definition}) + O(\text{initialization}) \\
 &+ O(\text{function evaluation}) \\
 &+ O(\text{Position updating in detour foraging}) \\
 &+ O(\text{Position updating in random hiding}) \\
 &+ O(\text{Position updating in Quantum1}) \\
 &+ O(\text{Position updating in Quantum2}) \\
 &= O\left(1 + n + Tn + \frac{1}{2}Tnd + \frac{1}{2}Tnd + \frac{1}{2}Tnd + \frac{1}{2}Tnd\right) \\
 &\cong O(2Tnd + Tn + n)
 \end{aligned}$$

5 Simulation results and discussion

Performance analysis of the QARO algorithm.

5.1 Benchmark functions

All techniques have been run under the similar situations so that a reasonable assessment is made. The number of search agents has been 50, while the maximum iteration equal to 200, and independent runs is 20 times to avoid the stochastic nature of the algorithms. The parameters specified in the original reference were employed for each method. Table 2 displays the parameter configurations for these techniques. These methods were compared using a laptop with a 2.9 GHz frequency, and the operating system used was Windows 10. The MATLAB 2016a platform was used to execute the techniques. The competence and the precision of the proposed QARO algorithm are evaluated on 23 benchmark functions based on different statistical measurements such as the best, average, median, worst values, standard deviation (std) and rank for the solutions achieved using the conventional ARO algorithm and other

Table 4 The statistical results of 23 benchmark functions

Function	QARO	ARO	SDO	EO	GWO
F1					
Best	8.37E−50	1.59E−26	1.39E−55	2.38E−18	4.47E−12
Average	1.3E−47	1.07E−21	1.37E−51	1.69E−17	3.12E−11
Median	4.96E−48	4.68E−23	3.74E−54	1.09E−17	2.46E−11
Worst	6E−47	7.08E−21	8.43E−51	6.39E−17	8.73E−11
Std	1.8E−47	2.18E−21	2.74E−51	1.72E−17	2.31E−11
Rank	2	3	1	4	5
F2					
Best	1.84E−27	1.34E−14	1.83E−29	5.21E−11	1.42E−07
Average	1.45E−26	1.15E−12	3.76E−25	1.63E−10	2.77E−07
Median	1.12E−26	1.22E−13	1.13E−26	1.42E−10	2.66E−07
Worst	7.39E−26	1.78E−11	3.98E−24	4.47E−10	4.78E−07
Std	1.57E−26	3.94E−12	9.1E−25	1.03E−10	9.9E−08
Rank	1	3	2	4	5
F3					
Best	1.11E−22	4.28E−21	6.27E−46	7.16E−05	0.008462
Average	2.57E−15	5.08E−15	6.91E−34	0.012312	0.610441
Median	4.82E−17	6.99E−17	1.4E−39	0.001321	0.185412
Worst	3.46E−14	6.41E−14	1.38E−32	0.149211	3.567009
Std	7.86E−15	1.51E−14	3.09E−33	0.034853	0.827115
Rank	2	3	1	4	5
F4					
Best	1.54E−18	8.35E−13	1.11E−26	1.78E−05	0.002608
Average	4.56E−17	2.6E−09	4.52E−23	0.000138	0.008
Median	3.07E−17	7.79E−10	1.14E−23	5.67E−05	0.007092
Worst	1.58E−16	2.28E−08	1.94E−22	0.000648	0.016667
Std	4.44E−17	5.09E−09	6.34E−23	0.000166	0.003845
Rank	2	3	1	4	5
F5					
Best	0.353027	0.048127	27.90967	25.6266	25.92515
Average	9.945439	2.57084	28.65096	26.26018	27.18903
Median	4.827879	1.069097	28.74726	26.11165	27.09814
Worst	27.77828	16.26736	28.98699	27.83945	28.79035
Std	10.83826	3.783419	0.295026	0.498931	0.72182
Rank	2	1	5	3	4
F6					
Best	0.016838	0.009568	0.039957	0.000201	0.252254
Average	0.034403	0.044563	2.568541	0.000497	0.647554
Median	0.031701	0.039666	2.038779	0.000417	0.611378
Worst	0.062803	0.098375	7.250251	0.001518	1.172757
Std	0.012711	0.026373	1.852701	0.000297	0.280888
Rank	2	3	5	1	4
F7					
Best	3.6E−05	3.22E−05	8.66E−05	0.000243	0.001477
Average	0.000467	0.001407	0.002356	0.001908	0.004433
Median	0.000393	0.00115	0.001136	0.001826	0.003685
Worst	0.001337	0.003564	0.013813	0.005511	0.01033
Std	0.000311	0.001071	0.003331	0.001275	0.002554

Table 4 (continued)

Function	QARO	ARO	SDO	EO	GWO
Rank	1	2	4	3	5
F8					
Best	-1763.41	-9902.5	-1655	-1796.54	-1495.31
Average	-1636.35	-9268.23	-1312.83	-1743.05	-1245.57
Median	-1664.54	-9276.94	-1385.86	-1742.67	-1224.18
Worst	-1378.02	-7798.04	-598.802	-1681.91	-1123.85
Std	113.3716	494.4779	294.008	28.37994	104.0153
Rank	3	1	4	2	5
F9					
Best	0	0	4.33E-30	5.68E-14	1.062467
Average	0	0	1.75E-22	0.049752	9.801018
Median	0	0	4.17E-25	1.14E-13	9.824713
Worst	0	0	3.02E-21	0.99503	24.96968
Std	0	0	6.75E-22	0.222496	5.565812
Rank	1	1	3	4	5
F10					
Best	8.88E-16	3.29E-14	8.88E-16	20	20.76487
Average	0.183959	5.19E-12	8.88E-16	20.00003	20.92344
Median	8.88E-16	1.26E-12	8.88E-16	20	20.94465
Worst	3.679179	5.25E-11	8.88E-16	20.00065	21.06309
Std	0.822689	1.17E-11	0	0.000145	0.083433
Rank	3	2	1	4	5
F11					
Best	0	0	0	0	6.56E-13
Average	0	0	0	1.39E-16	0.009891
Median	0	0	0	0	4.55E-12
Worst	0	0	0	2.22E-15	0.055407
Std	0	0	0	4.92E-16	0.015766
Rank	1	1	1	4	5
F12					
Best	0.000481	0.000211	0.001152	5.41E-06	0.006066
Average	0.001037	0.002555	0.23467	1.46E-05	0.026151
Median	0.000968	0.002594	0.067805	1.46E-05	0.023474
Worst	0.002366	0.004551	1.492821	3.77E-05	0.047176
Std	0.000479	0.001218	0.352063	8.5E-06	0.013414
Rank	2	3	5	1	4
F13					
Best	0.010677	0.005253	0.046216	0.000219	0.09955
Average	0.033325	0.038605	1.867552	0.039624	0.613832
Median	0.030899	0.020631	1.934246	0.001307	0.609981
Worst	0.068387	0.218513	2.999924	0.207579	1.044
Std	0.014292	0.051532	0.961284	0.072678	0.280029
Rank	1	2	5	3	4
F14					
Best	0.998004	0.998004	0.998004	0.998004	0.998004
Average	0.998004	0.998004	3.494696	0.998004	3.892106
Median	0.998004	0.998004	1.495017	0.998004	2.982105
Worst	0.998004	0.998004	12.67051	0.998004	12.67051

Table 4 (continued)

Function	QARO	ARO	SDO	EO	GWO
Std	1.84E-16	2.97E-16	3.953203	1.84E-16	3.727681
Rank	2	2	4	1	5
F15					
Best	0.000308	0.000308	0.000307	0.000308	0.00031
Average	0.000325	0.000441	0.00067	0.004398	0.003547
Median	0.000313	0.000404	0.000527	0.00035	0.000546
Worst	0.000405	0.000694	0.002121	0.020363	0.020363
Std	2.55E-05	0.000131	0.000473	0.008192	0.007255
Rank	1	2	3	5	4
F16					
Best	- 1.03163	- 1.03163	- 1.03163	- 1.03163	- 1.03163
Average	- 1.03163	- 1.03163	- 1.03005	- 1.03163	- 1.03158
Median	- 1.03163	- 1.03163	- 1.03163	- 1.03163	- 1.03163
Worst	- 1.03163	- 1.03163	- 1.00046	- 1.03163	- 1.03063
Std	5.19E-13	2.5E-12	0.006966	1.76E-16	0.000223
Rank	2	3	5	1	4
F17					
Best	0.397887	0.397887	0.397887	0.397887	0.397888
Average	0.397887	0.397887	0.397987	0.397887	0.397891
Median	0.397887	0.397887	0.397887	0.397887	0.397891
Worst	0.397887	0.397887	0.399795	0.397887	0.397897
Std	0	1.28E-10	0.000426	0	3.01E-06
Rank	1	3	5	1	4
F18					
Best	3	3	3	3	3
Average	3	3	4.371758	3	3.000068
Median	3	3	3	3	3.000036
Worst	3	3	30.41145	3	3.000238
Std	1.49E-15	1.16E-15	6.129111	2.16E-15	6.53E-05
Rank	1	1	5	3	4
F19					
Best	- 0.30048	- 3.86278	- 0.30048	- 0.30048	- 0.30048
Average	- 0.30048	- 3.86278	- 0.2893	- 0.30048	- 0.30048
Median	- 0.30048	- 3.86278	- 0.30038	- 0.30048	- 0.30048
Worst	- 0.30048	- 3.86278	- 0.19165	- 0.30048	-0.30048
Std	1.14E-16	3.73E-15	0.026531	1.14E-16	1.14E-16
Rank	2	1	5	2	2
F20					
Best	-3.322	-3.322	-3.322	-3.322	-3.32198
Average	-3.32198	-3.31597	-3.09697	-3.20051	-3.22876
Median	-3.322	-3.322	-3.2031	-3.322	-3.26239
Worst	-3.3218	-3.2031	-0.89904	-1.84092	-2.84039
Std	4.68E-05	0.026567	0.550986	0.327557	0.125558
Rank	1	2	5	4	3
F21					
Best	- 10.1512	- 10.1532	- 10.1532	- 10.1532	- 10.1502
Average	- 7.3638	- 10.1187	- 8.703	- 9.26724	- 8.51218
Median	- 6.77544	- 10.1532	- 10.1532	- 10.1532	- 10.1413

Table 4 (continued)

Function	QARO	ARO	SDO	EO	GWO
Worst	- 5.0552	- 9.81141	- 4.99677	- 2.63047	- 2.62918
Std	2.409973	0.090338	2.23952	2.210886	2.963153
Rank	5	1	3	2	4
F22					
Best	- 10.4029	- 10.4029	- 10.4029	- 10.4029	- 10.4024
Average	- 9.19054	- 10.1364	- 8.45822	- 8.27887	- 10.0134
Median	- 10.4025	- 10.4029	- 10.4029	- 10.4029	- 10.3959
Worst	- 5.08767	- 5.07631	- 1.0677	- 5.08767	- 2.76526
Std	2.128761	1.191013	3.128689	2.668997	1.706042
Rank	3	1	4	5	2
F23					
Best	- 10.5364	- 10.5364	- 10.5364	- 10.5364	- 10.5348
Average	- 10.2579	- 10.1522	- 7.90449	- 9.32552	- 9.74305
Median	- 10.5364	- 10.5364	- 10.5357	- 10.5364	- 10.5274
Worst	- 5.12848	- 3.83543	- 3.79083	- 3.83543	- 2.42135
Std	1.207807	1.502943	3.015319	2.502342	2.418464
Rank	1	2	5	4	3
Average rank	1.826087	2	3.565217	3	4.173913
Final ranking	1	2	4	3	5

Algorithms Performance for 23 Benchmark Function

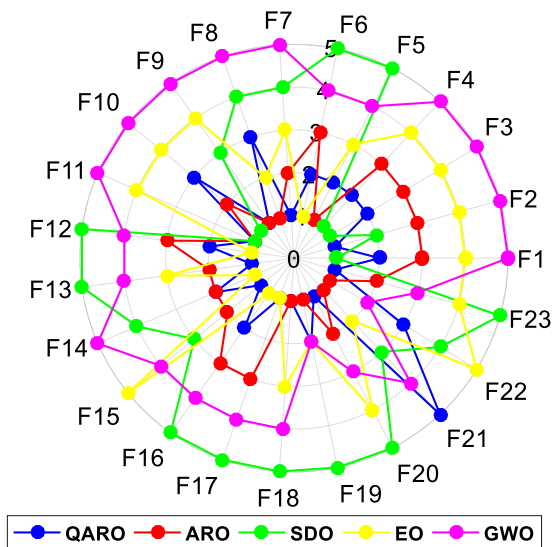


Fig. 3 Radar chart for ranks among all compared algorithms

recent techniques such as the supply-demand-based optimization (SDO) (Zhao et al. 2019), the Equilibrium optimizer (EO) (Faramarzi et al. 2020), and the Grey wolf optimizer (GWO) (Mirjalili et al. 2014).

These benchmark functions comprise three types of test functions: unimodal, multimodal, and low-dimensional

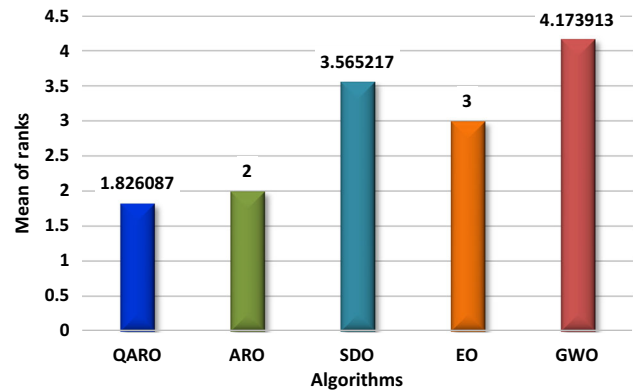


Fig. 4 Mean ranks obtained by tied rank test for 23 functions using various algorithms

multimodal test functions (Fan et al. 2021). The mathematical formulation for these test functions can be found in Table 3. The first group of test functions belongs to the unimodal family, and contains only one global optimum, without any local optima. These test functions are highly suitable for evaluating algorithm convergence speed and exploitation capabilities. The second group, which belongs to the multimodal family, consists of test functions with multiple local solutions in addition to the global optimum. These test functions are useful for testing an algorithm's

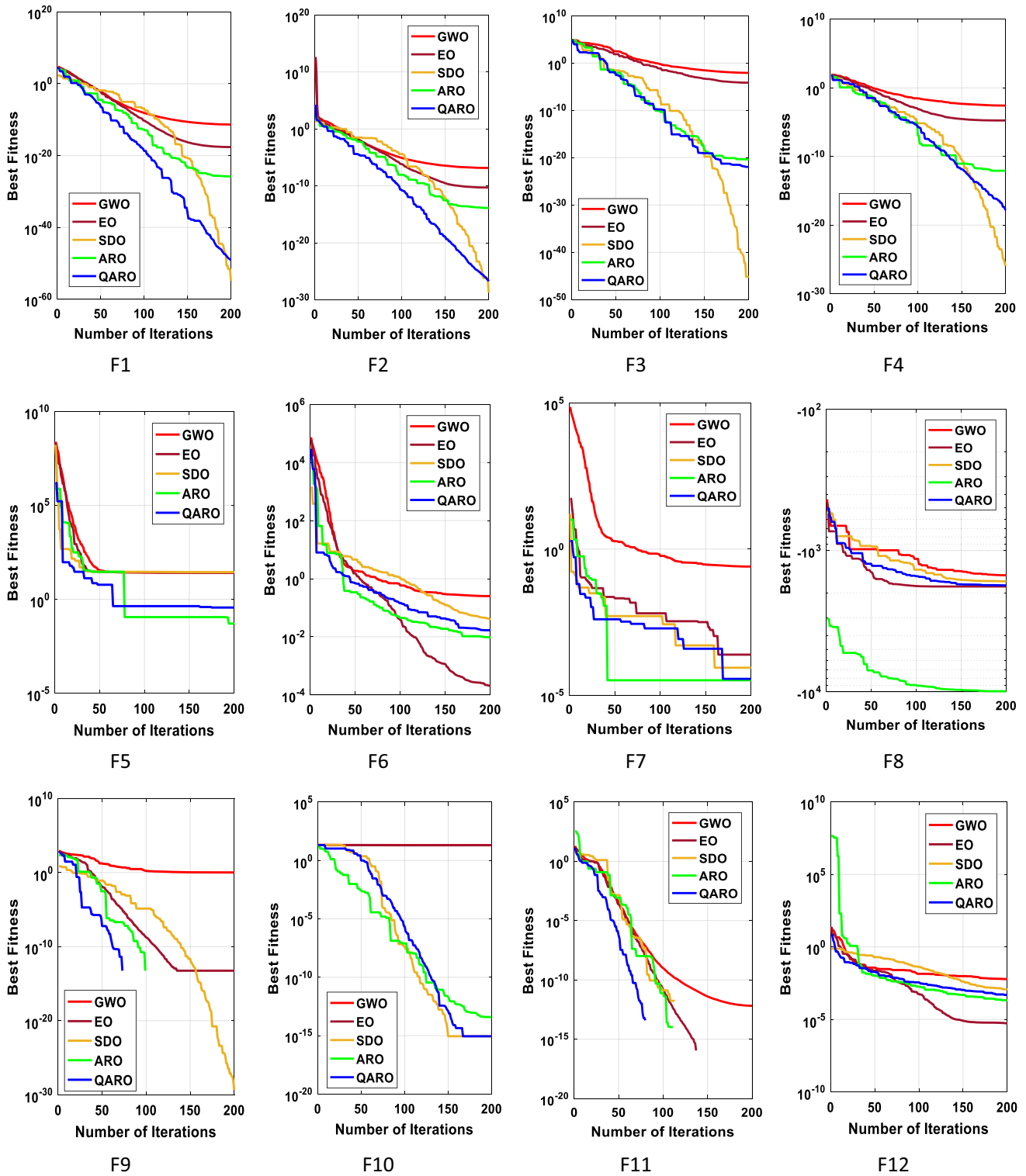


Fig. 5 The convergence curves of all algorithms for 23 benchmark functions

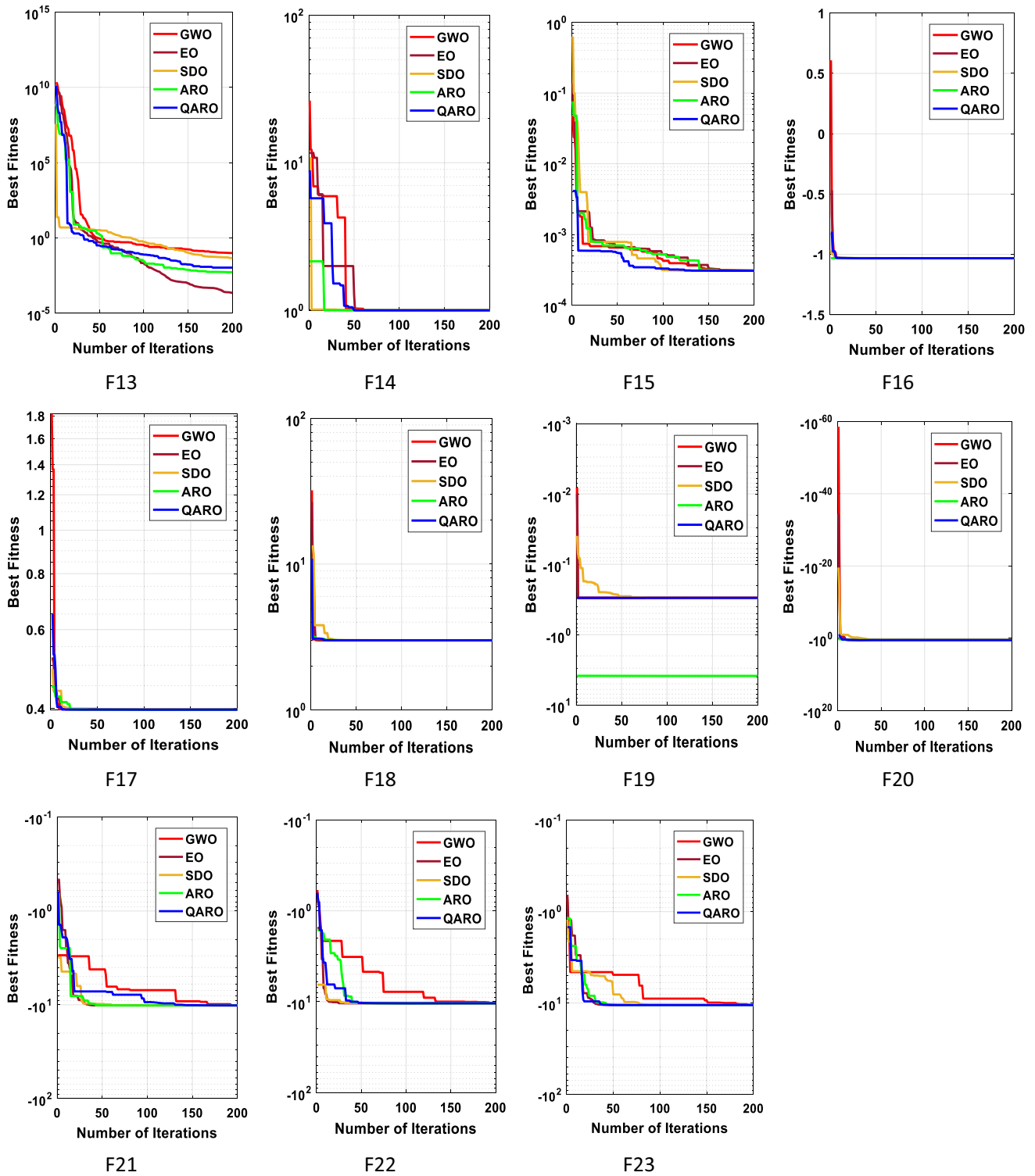


Fig. 5 continued

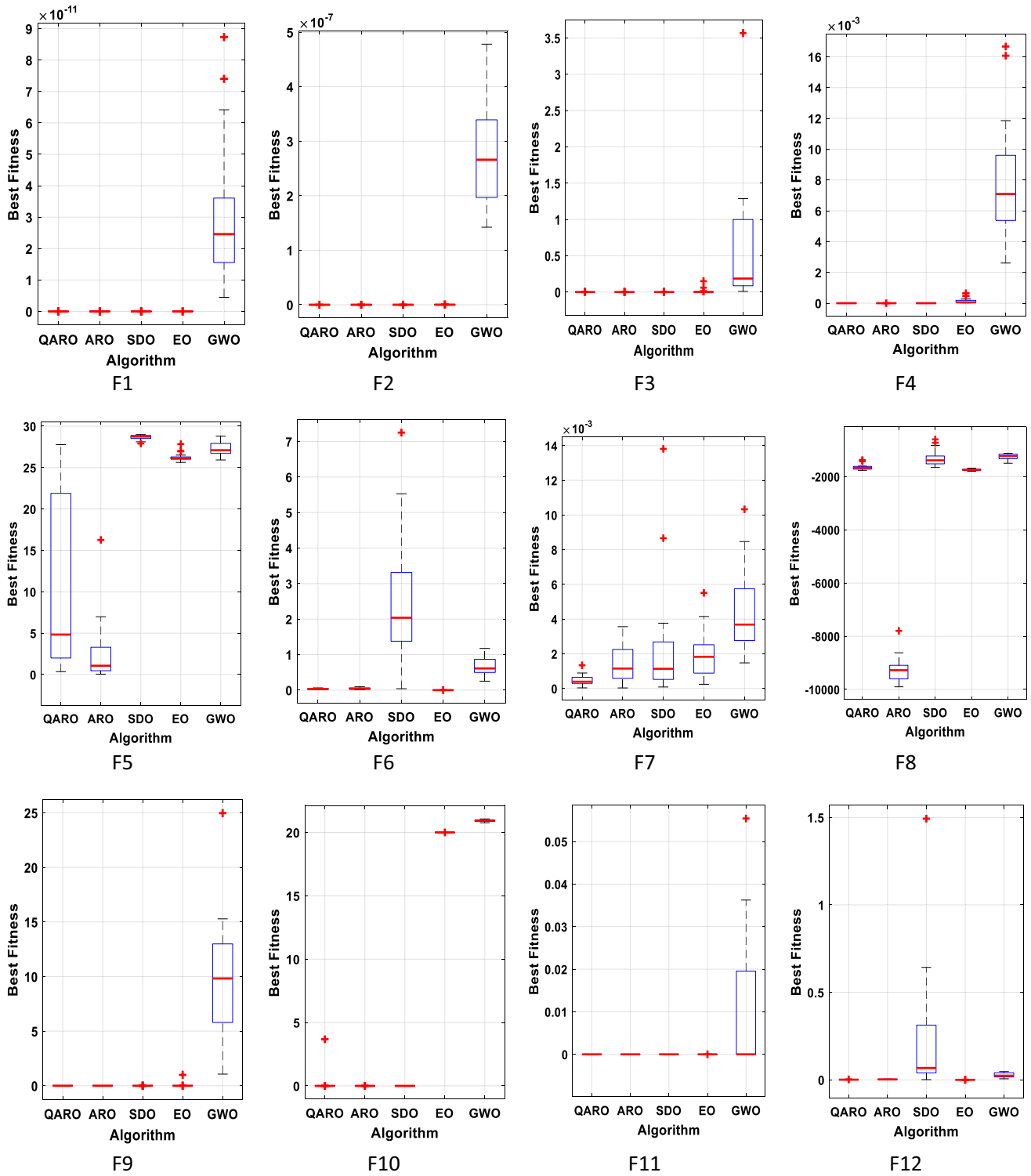


Fig. 6 Boxplots for all algorithms for 23 benchmark functions

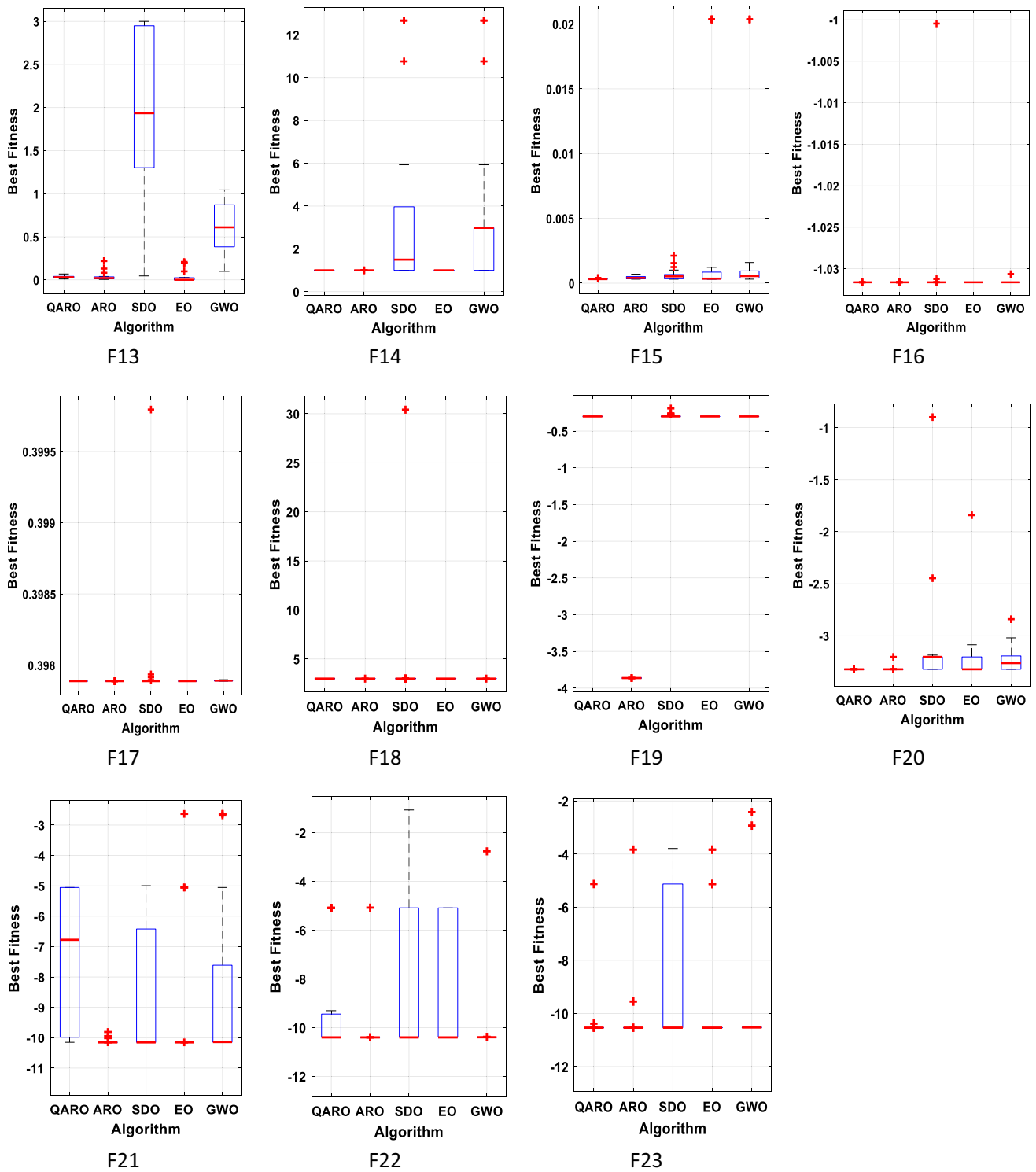


Fig. 6 continued

Table 5 Table Statistical comparisons of Wilcoxon signed-rank test for QARO versus ARO, SDO, EO, and GWO

Function	QARO versus ARO				QARO versus SDO				QARO versus EO				QARO versus GWO			
	R+	R-	p value	H0	R+	R-	p value	H0	R+	R-	p value	H0	R+	R-	p value	H0
F1	210	0	8.86E-05	No	0	210	8.86E-05	No	210	0	8.86E-05	No	210	0	8.86E-05	No
F2	210	0	8.86E-05	No	142	68	0.167184	Yes	210	0	8.86E-05	No	210	0	8.86E-05	No
F3	112	98	0.793839	Yes	0	210	8.86E-05	No	210	0	8.86E-05	No	210	0	8.86E-05	No
F4	210	0	8.86E-05	No	0	210	8.86E-05	No	210	0	8.86E-05	No	210	0	8.86E-05	No
F5	27	183	0.003592	No	210	0	8.86E-05	No	197	13	0.000593	No	203	7	0.000254	No
F6	147	63	0.116888	Yes	210	0	8.86E-05	No	0	210	8.86E-05	No	210	0	8.86E-05	No
F7	194	16	0.000892	No	186	24	0.002495	No	204	6	0.000219	No	210	0	8.86E-05	No
F8	0	210	8.86E-05	No	210	0	8.86E-05	No	11	199	0.000449	No	209	1	0.000103	No
F9	0	0	1	Yes	210	0	8.86E-05	No	210	0	7.61E-05	No	210	0	8.86E-05	No
F10	154	56	0.067355	Yes	0	15	0.0625	Yes	210	0	2.98E-05	No	210	0	8.86E-05	No
F11	0	0	1	Yes	0	0	1	Yes	21	0	0.03125	No	210	0	8.86E-05	No
F12	196	14	0.000681	No	210	0	8.86E-05	No	0	210	8.86E-05	No	210	0	8.86E-05	No
F13	76	134	0.278965	Yes	210	0	8.86E-05	No	75	135	0.262722	Yes	210	0	8.86E-05	No
F14	12	3	0.375	Yes	103.5	1.5	0.000366	No	0	6	0.25	Yes	210	0	8.86E-05	No
F15	193	17	0.001019	No	193	17	0.001019	No	180	30	0.005111	No	204	6	0.000219	No
F16	61.5	43.5	0.594238	Yes	70.5	49.5	0.570801	Yes	0	45	0.003906	No	210	0	8.86E-05	No
F17	153	0	0.000291	No	28	0	0.015625	No	0	0	1	Yes	210	0	8.86E-05	No
F18	18	48	0.226563	Yes	168.5	2.5	0.000286	No	64	56	1	Yes	210	0	8.86E-05	No
F19	0	210	3.67E-05	No	210	0	8.86E-05	No	0	0	1	Yes	0	0	1	Yes
F20	97	113	0.765198	Yes	200	10	0.00039	No	132	78	0.313463	Yes	195	15	0.00078	No
F21	10	200	0.00039	No	47	163	0.030365	No	30	180	0.005111	No	53	157	0.052222	Yes
F22	44	166	0.022769	No	115	95	0.708905	Yes	104	106	0.97022	Yes	98	112	0.793839	Yes
F23	57	153	0.073138	Yes	166	44	0.022769	No	68	142	0.167184	Yes	189	21	0.001713	No
w/t/I	12/11/ 0	18/5/ 0	15/8/0	20/3/ 0												

ability to avoid local optima and explore alternative solutions. The composite test functions are a combination of rotated, shifted, biased, and merged versions of various unimodal and multimodal test functions.

5.1.1 Comparison simulation results

The comparisons for these algorithms are presented in Table 4. From Table 4, it is noticed that the proposed QARO algorithm achieves best results on the most of these types of functions in all values. The comparison of techniques in these functions is according to the average value. These functions are compared based on their mean values using a technique called Tied rank (TR). This rank-based approach assigns ranks to the techniques according to their average values, with the technique with the smallest

average value being allocated rank 1, and so on. The technique with the lowest TR value is considered the most effective compared to the other algorithms (El-Dabah et al. 2023; Wu et al. 2019). The statistical results of the tied rank on 23 benchmark functions are shown in Table 4. After Table 4 is inspected; the applied techniques are sorted. It is seen from the ranking order that the QARO algorithm outperforms the other compared techniques on 23 function problems. ARO and EO displays robust effectiveness that are the second and third optimal. Figure 3 displays the ranking of all compared algorithms for each function, using a radar chart. The average of these ranks is presented in Fig. 4. Upon examining Fig. 4, it becomes evident that QARO has the lowest average rank value, implying that it ranks first among all algorithms. This underscores QARO as the top-performing optimizer in

Table 6 Anova Kruskal–Wallis test

Function	Source	Sum of square	Degree of freedom	Mean square	Chi-sq	Prob > Chi-sq
F1	Columns	80,000	4	20,000	95.05407	1.11E−19
	Error	3321	95	34.95789	–	–
	Total	83,321	99	–	–	–
F2	Columns	76,019.6	4	19,004.9	90.32032	1.13E−18
	Error	7305.4	95	76.89895	–	–
	Total	83,325	99	–	–	–
F3	Columns	75,427.4	4	18,856.85	89.61671	1.59E−18
	Error	7897.6	95	83.13263	–	–
	Total	83,325	99	–	–	–
F4	Columns	80,000	4	20,000	95.0495	1.11E−19
	Error	3325	95	35	–	–
	Total	83,325	99	–	–	–
F5	Columns	67,210.4	4	16,802.6	79.85394	1.87E−16
	Error	16,114.6	95	169.6274	–	–
	Total	83,325	99	–	–	–
F6	Columns	73,091.3	4	18,272.83	86.84115	6.17E−18
	Error	10,233.7	95	107.7232	–	–
	Total	83,325	99	–	–	–
F7	Columns	38,493.3	4	9623.325	45.73461	2.8E−09
	Error	44,831.7	95	471.9126	–	–
	Total	83,325	99	–	–	–
F8	Columns	72,703.3	4	18,175.83	86.38016	7.73E−18
	Error	10,621.7	95	111.8074	–	–
	Total	83,325	99	–	–	–
F9	Columns	76,000	4	19,000	96.5327	5.38E−20
	Error	1942.5	95	20.44737	–	–
	Total	77,942.5	99	–	–	–
F10	Columns	73,353.1	4	18,338.28	91.70874	5.71E−19
	Error	5831.9	95	61.38842	–	–
	Total	79,185	99	–	–	–
F11	Columns	42,160	4	10,540	84.23066	2.21E−17
	Error	7392.5	95	77.81579	–	–
	Total	49,552.5	99	–	–	–
F12	Columns	72,315.5	4	18,078.88	85.91941	9.68E−18
	Error	11,009.5	95	115.8895	–	–
	Total	83,325	99	–	–	–
F13	Columns	63,122.7	4	15,780.68	74.99727	2E−15
	Error	20,202.3	95	212.6558	–	–
	Total	83,325	99	–	–	–
F14	Columns	51,081.2	4	12,770.3	64.21107	3.77E−13
	Error	27,675.3	95	291.3189	–	–
	Total	78,756.5	99	–	–	–
F15	Columns	20,676.4	4	5169.1	24.56661	6.15E−05
	Error	62,646.6	95	659.4379	–	–
	Total	83,323	99	–	–	–
F16	Columns	49,282.7	4	12,320.68	61.16204	1.65E−12
	Error	30,488.8	95	320.9347	–	–
	Total	79,771.5	99	–	–	–

Table 6 (continued)

Function	Source	Sum of square	Degree of freedom	Mean square	Chi-sq	Prob > Chi-sq
F17	Columns	47,428.93	4	11,857.23	68.35383	5.05E-14
	Error	21,264.58	95	223.8376	–	–
	Total	68,693.5	99	–	–	–
F18	Columns	59,551.25	4	14,887.81	71.31498	1.2E-14
	Error	23,118.25	95	243.35	–	–
	Total	82,669.5	99	–	–	–
F19	Columns	64,000	4	16,000	97.15109	3.97E-20
	Error	1218	95	12.82105	–	–
	Total	65,218	99	–	–	–
F20	Columns	31,231.6	4	7807.9	37.11687	1.7E-07
	Error	52,070.9	95	548.1147	–	–
	Total	83,302.5	99	–	–	–
F21	Columns	36,674.1	4	9168.525	43.61925	7.7E-09
	Error	46,562.9	95	490.1358	–	–
	Total	83,237	99	–	–	–
F22	Columns	15,575.6	4	3893.9	18.51611	0.000978
	Error	67,702.4	95	712.6568	–	–
	Total	83,278	99	–	–	–
F23	Columns	29,166.8	4	7291.7	34.66985	5.43E-07
	Error	54,119.2	95	569.6758	–	–
	Total	83,286	99	–	–	–

Table 7 Parameters of the three CDG units (case study 1)

<i>i</i>	Generation coefficients			Limits		
	a_i (\$/kW ² h)	b_i (\$/KW h)	$P_{i,min}$ (KW)	$P_{i,max}$ (KW)	DR _{<i>i</i>} (KW/h)	UR _{<i>i</i>} (KW/h)
1	0.06	0.5	0	4	3	3
2	0.03	0.25	0	6	5	5
3	0.04	0.3	0	9	8	8

Table 8 Customers data (Case study 1)

<i>J</i>	θ_j	$K_{1,j}$	$K_{2,j}$	P_{CM_j} (kWh)
1	0	1.079	1.32	30
2	0.45	1.378	1.36	35
3	0.9	1.847	1.64	40

the comparison, based on the tied rank approach. This outcome further validates that our method can efficiently discover the global optimum for various problems. It is concluded from this discussion that the QARO technique becomes an effective algorithm for solving these types of problems. The convergence characteristics of these

algorithms for those functions are displayed in Fig. 5. For more investigation on the performance of the proposed algorithm, a boxplot of outcomes for each algorithm and objective function is presented in Fig. 6 also displays that the boxplots of proposed QARO algorithm for most of the functions are narrow and among the smallest values.

5.1.2 Wilcoxon’s rank test results

The Wilcoxon signed-rank test is a nonparametric test used to determine whether the median of a paired sample differs significantly from a hypothesized value. It is commonly used in situations where the data is not normally distributed or the assumptions for a paired *t* test are not met. To

Table 9 Power interruptibility $\lambda_{j,t}$ data for case study 1

Time (h)	$\lambda_{1,t}$ (\$)	$\lambda_{2,t}$ (\$)	$\lambda_{3,t}$ (\$)
$t = 1$	1.57	3.70	2.70
$t = 2$	1.4	2.70	1.90
$t = 3$	2.2	3.20	1.80
$t = 4$	3.76	2.60	1.90
$t = 5$	4.5	3.80	2.30
$t = 6$	4.7	1.70	0.70
$t = 7$	5.04	2.30	1.40
$t = 8$	5.35	1.50	0.50
$t = 9$	6.7	4.30	2.90
$t = 10$	6.16	4.60	1.60
$t = 11$	6.38	3.50	4.30
$t = 12$	6.82	4.20	4.80
$t = 13$	7.3	4.30	5.10
$t = 14$	7.8	6.30	5.40
$t = 15$	8.5	3.50	5.50
$t = 16$	7.1	5.30	6.10
$t = 17$	6.8	5.30	5.60
$t = 18$	6.3	6.10	6.30
$t = 19$	5.8	2.60	4.50
$t = 20$	4.2	3.60	4.20
$t = 21$	3.8	4.20	3.90
$t = 22$	3.01	3.80	3.20
$t = 23$	2.53	2.30	2.80
$t = 24$	1.42	3.80	4.20

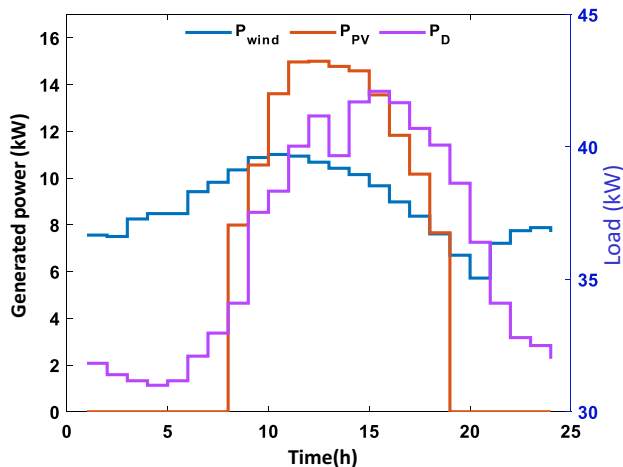


Fig. 7 Initial demand load and the power generated from PV and WT

compare the performance of any two algorithms, the Wilcoxon signed rank test is carried out. This involves

gathering all fitness values over 30 runs of the objective for both algorithms, computing the sum of ranks for runs in which one algorithm outperforms the other, and calculating the p value to determine the significance of the results. Table 5 presents the results obtained using the Wilcoxon signed rank test. The column H_0 defines whether the null hypothesis is valid or not. If H_0 is valid with a significance level of $\alpha = 0.05$, the performance of two methods is statistically the same for the study case (Biswas et al. 2018; Derrac et al. 2011).

To compare the performance of two algorithms, the following steps were taken:

- Gathered all fitness values for both algorithms over 30 runs of the objective in a case study.
- Calculated $R+$, the sum of ranks for runs in which algorithm 'A' outperforms algorithm 'B'.
- Calculated $R-$, the sum of ranks for runs in which algorithm 'B' outperforms algorithm 'A'.
- Calculated the p value, which indicates the significance of results in a statistical hypothesis test. A smaller p value suggests stronger evidence against the null hypothesis H_0 .

Table 5 shows that QARO outperforms all other competitors for most functions, indicating a significant improvement in performance.

5.1.3 Kruskal–Wallis statistical analysis of the results

The Kruskal–Wallis test is a widely recognized statistical test that takes into account the overall rankings of multiple variables across different datasets (Gupta et al. 2020). The QARO algorithm exhibits a significantly better median rank compared to the other groups, as indicated by the ANOVA Kruskal–Wallis test results presented in Table 6. The probability value verified by the chi-square test further supports this finding. Based on the nonparametric tests conducted, it can be inferred that the QARO algorithm demonstrates greater precision and accuracy than the algorithms it was compared against (Table 6).

5.2 Real-world application

This section presents the numerical analysis and result of the proposed QARO to solve the EM problem to evaluate its performance. QARO determines the optimal operating conditions for the MG resources and the optimal scheduling for DRP operation. The generation data for WT and solar PV are given in Nwulu and Xia (2017), and it is assumed that their operational cost is negligible. The cost

Table 10 Comparison of the EM problem for case study 1

Technique	Total operating cost (\$)			
	Worst	Best	Mean	STD
PSO (Moghaddam et al. 2011)	699.47	623.24	665.1084	15.96
JAYA (Warid et al. 2016)	804.37	689.77	743.8394	31.25
INFO (Ahmadianfar et al. 2022)	642.35	520.56	580.8188	31.607
SO (Hashim and Hussien 2022)	782.91	619.70	692.99	42.67
ARO (Wang et al. 2022)	566.05	523.92	540.5792	11.14
QARO	549.6943	517.065	530.9362	9.27

Bold value indicate the best results

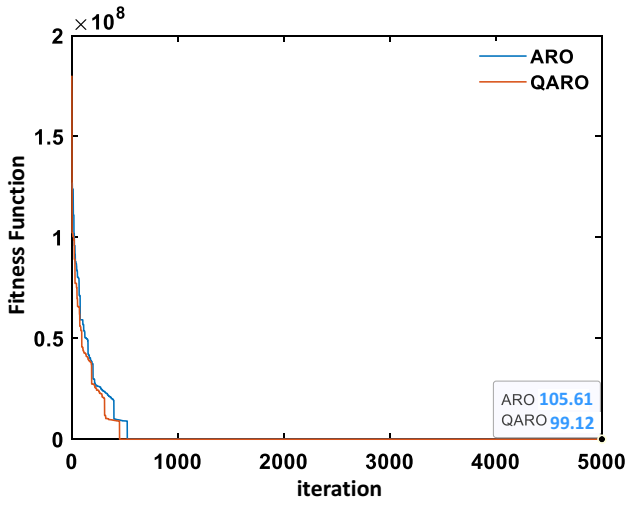


Fig. 8 The convergence characteristics of ARO and QARO

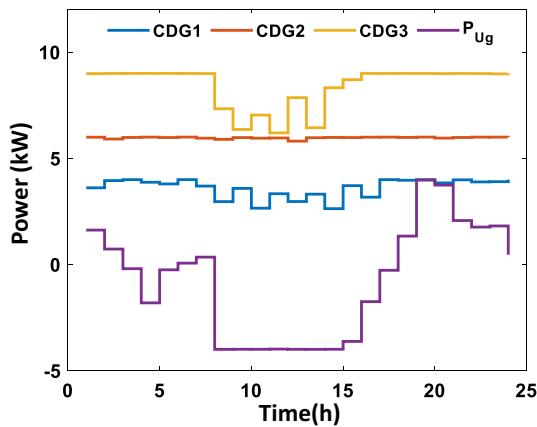


Fig. 9 The power generated from CDG and transacted with the grid

function’s coefficients of CDG are used in Alamir et al. (2022a). To evaluate the performance of the proposed QARO in solving the EMS problem, two different MG test systems based on the proposed MG architecture shown in Fig. 1 have been formulated and simulated.

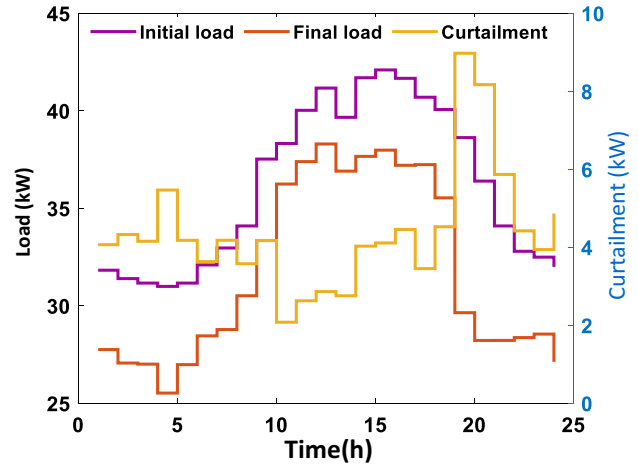


Fig. 10 The initial and final load and total curtailment for case study 1

Table 11 Comparison of the EM problem for case study 1

j	Saving (kWh)	Incentive (\$)
1	29.99001	83.79387
2	34.98977	119.5918
3	39.99829	164.275
Total	104.97	367.6615

Case Study 1

The grid-connected MG’s architecture in the first case study consists of three CDG units, one WT unit, one Solar PV unit, and three customers. The parameters of the three CDGs, including fuel cost coefficients, generation limits, and ramping up and down limits, are provided in Table 7. Data of the three residential customers included cost coefficients, θ_j , and the daily power curtailment are detailed in Table 8. Power interruptibility ($\lambda_{j,t}$) for the three customers is provided in Table 9. The hourly WT and PV

Fig. 11 Comparison of all studied optimization techniques for case study 1

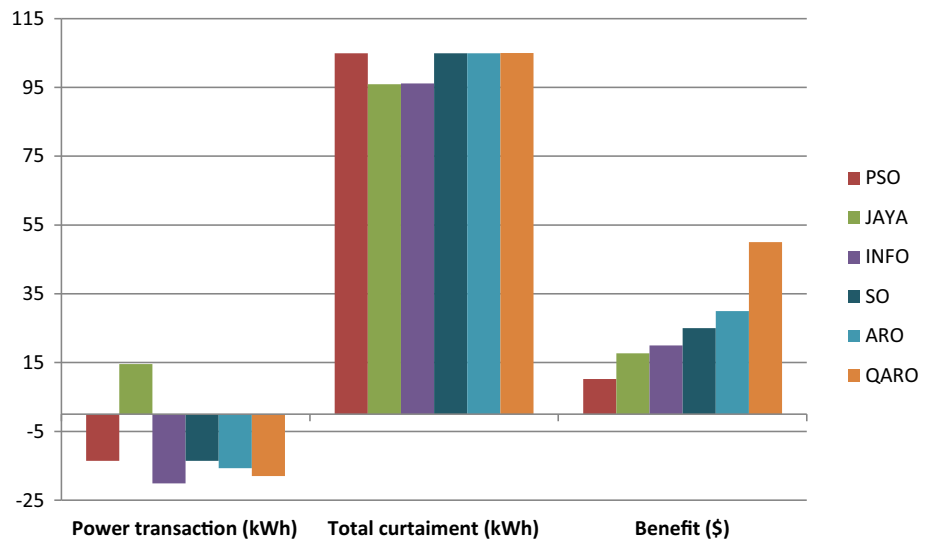


Table 12 Customers data (Case study 2)

J	θ	$K_{1,j}$	$K_{2,j}$	P_{CM_j} (MWh)
1	0	1.847	11.64	180
2	0.14	1.378	11.63	230
3	0.26	1.079	11.32	310
4	0.37	0.9124	11.5	390
5	0.55	0.8794	11.21	440
6	0.84	1.378	11.63	530
7	1	1.5231	11.5	600

power generation, as well as the initial load demand ($P_{D,t}$) are shown in Fig. 7. It is also assumed that MGO has previous information about its own daily budget of \$500.

All simulations were conducted on MATLAB 2021b on an i7-2.9 GHz computer with 8 GB of RAM. The results of 30 independent runs of the proposed MG architecture are compared using the proposed QARO, ARO (Wang et al. 2022), PSO (Moghaddam et al. 2011), JAYA (Warid et al. 2016), INFO (Ahmadianfar et al. 2022), and SO (Hashim and Hussien 2022). The results are presented in Table 10. The proposed QARO has the best performance in terms of best, worst, mean and Standard deviation (STD) values. The best results for each algorithm are compared, and the results will be discussed. The convergence characteristics of the original algorithm ARO and the proposed QARO are shown in Fig. 8; it can be seen that the QARO has faster convergence characteristics and better performance in giving lower operating cost.

Using QARO, the power generated from the CDG units for the whole interval is shown in Fig. 9. The load demand before and after employing the DRP with the power curtailed from all customers as a response to the DR are shown in Fig. 10. A detailed customer curtailment and total incentive are given in Table 11. A comparison for all studied techniques in terms of total energy curtailment, power transaction, and MG benefit is shown in Fig. 11. Negative power transaction means the power sold to the utility grid is higher than that bought from it. The total curtailment during the day in case of using the proposed QARO is equal to 104.97 kWh. From the figure, the MG benefit is the highest in the case of QARO.

Case Study 2

To validate the scalability of the proposed QARO algorithm, a second test system with a larger MG is simulated; in this test system, the MG consists of 10 CDG, aggregated model for 10 WT units, aggregated model for 10 solar PV units, and seven residential consumers. The CDGs’ fuel cost coefficients and generation limits are given in Alamir et al. (2022a). The customers’ cost coefficients, θ_j , and the daily power curtailment are detailed in Table 12. The forecasted power from WT and PV units (Nwulu and Xia 2017) as well as the daily power interruptibility values for each customer (Kim and Kim 2019) are shown in Table 13.

In this case study simulated on MATLAB using different optimization techniques, the best results for the independent runs in each algorithm are compared; the total operating cost for all studied techniques is shown in Fig. 12; it can be noted that the proposed QARO achieved best operating cost over all the other techniques.

Table 13 WT and PV output power and customers' interruptibility values (Case study 2)

Time (h)	WT (MW)	PV (MW)	$\lambda_{1,t}$ (\$)	$\lambda_{2,t}$ (\$)	$\lambda_{3,t}$ (\$)	$\lambda_{4,t}$ (\$)	$\lambda_{5,t}$ (\$)	$\lambda_{6,t}$ (\$)	$\lambda_{7,t}$ (\$)
$t = 1$	113.44	0	27.61	28.3	28.79	26.93	27.6	27.38	27.3
$t = 2$	112.55	0	29.41	30.07	30.53	28.79	29.44	29.21	29.15
$t = 3$	123.76	0	28.24	28.87	29.28	27.66	28.33	28.08	28.02
$t = 4$	127.21	0	26.69	28.76	32.64	27.66	28.32	27.56	27.85
$t = 5$	127.33	0	29.01	32.24	37.15	31.2	31.66	30.62	31.16
$t = 6$	141.44	0	33.96	36.67	90.65	35.38	35.99	35.11	35.49
$t = 7$	147.39	0	83.97	89.46	83.79	85.71	87.7	85.79	86.4
$t = 8$	155.38	79.94	81.1	82.88	114.11	79.06	81.06	80.41	80.18
$t = 9$	168.33	105.69	110.6	112.93	76.09	107.72	110.44	109.59	109.25
$t = 10$	165.28	136.18	74.12	75.43	80.56	72.4	73.95	73.49	73.28
$t = 11$	164.23	149.75	78.95	80.19	67.76	77.29	78.93	78.39	78.2
$t = 12$	160.32	150	66.85	67.55	48.63	65.75	66.67	66.42	66.28
$t = 13$	156.31	147.89	47.98	48.58	65.07	47.1	47.39	47.49	47.33
$t = 14$	152.3	145.92	66.82	67.74	49.69	65.55	66.74	66.37	66.22
$t = 15$	145.05	135.65	48.5	49.35	50.87	47.41	48.47	48.13	48
$t = 16$	134.8	118.36	49.21	50.28	70.29	49.94	49.19	49.45	49.53
$t = 17$	125.64	101.71	66.65	69.36	67.19	66.05	67.71	66.8	66.85
$t = 18$	114.2	77.68	61.49	66.57	58.25	59.59	66.24	62.44	62.76
$t = 19$	100.63	0	56.19	57.67	59.89	54.48	56.53	55.73	55.58
$t = 20$	85.95	0	57.92	59.38	48.31	55.58	57.98	57.16	56.91
$t = 21$	108.26	0	49.16	49.68	53.36	48.31	48.96	48.81	48.69
$t = 22$	116.38	0	54	54.38	54.84	53.46	53.63	53.7	53.6
$t = 23$	118.33	0	34.37	34.67	34.96	33.98	34.21	34.19	34.13
$t = 24$	115.38	0	30.3	30.71	31	29.89	30.2	30.13	30.07

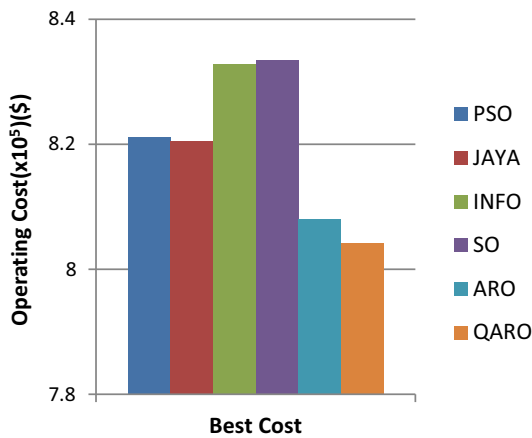


Fig. 12 Comparison for the operating cost for case study 2

Using QARO, the power generated from the CDG units for the whole interval is shown in Fig. 13. Customers' power curtailed and the incentive they get during the day are shown in Figs. 14 and 15 respectively. The load demand before and after employing the DRP with the sum of power curtailed from all customers as a response to the

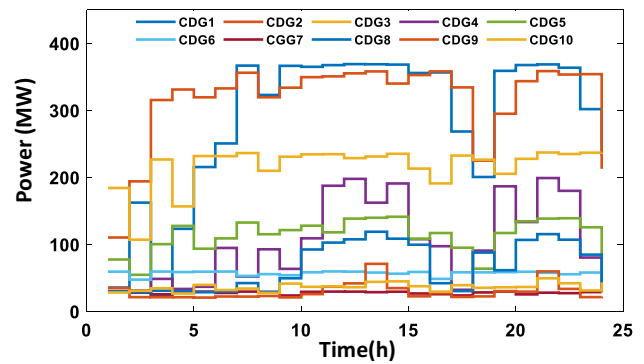


Fig. 13 Generated power from CDGs for case study 2

DR are shown in Fig. 16. A comparison for all studied techniques in terms of total energy curtailment, power transaction, and MG benefit is shown in Table 14. The total curtailment during the day in case of using the proposed QARO in case study 2 is equal to 2679.5 MWh. The MG's benefit using the proposed QARO algorithm is about 3000\$, which is higher than that in the case of PSO, INFO, SO, ARO.

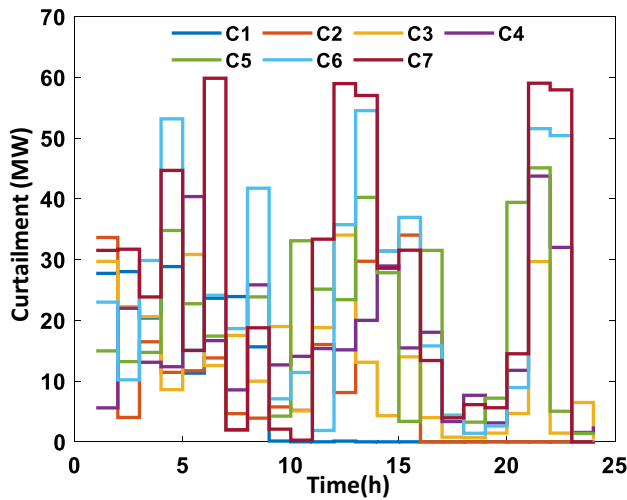


Fig. 14 Customers’ curtailment for case study 2

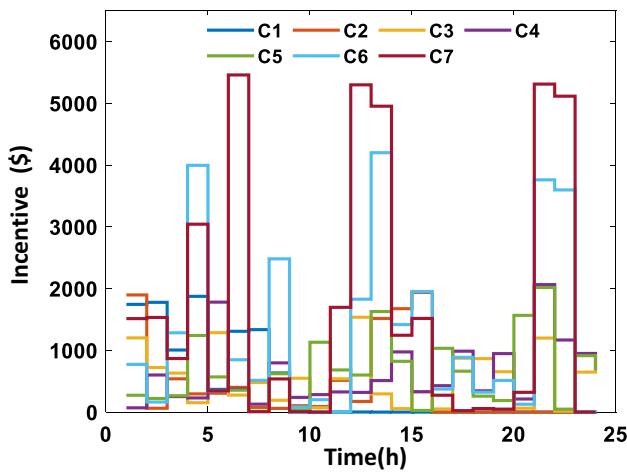


Fig. 15 Customers’ incentive for case study 2

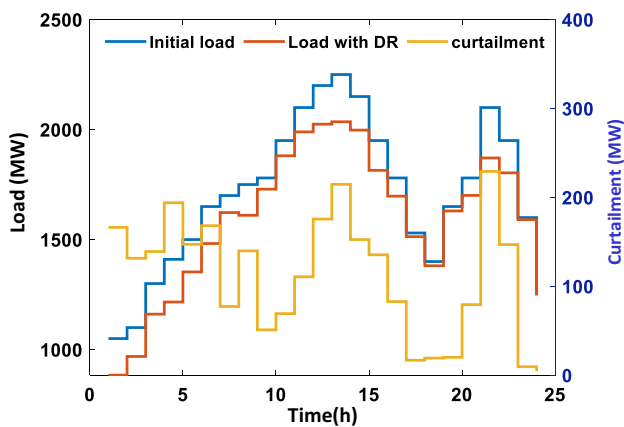


Fig. 16 The initial and final load and total curtailment for case study 2

6 Conclusion

This paper proposes a modified QARO algorithm to enhance the performance of the ARO algorithm by augmenting it with a quantum mechanism based on MCS simulation. The modified algorithm is applied to solve the EM problem of MG to minimize the operating costs and maximize the MGO benefit. The performance of the improved algorithm has been tested using 23 test bench functions and comparison with well-known techniques (e.g. SDO, EO, GWO and the original ARO), different statistical assessment are performed. TR technique used to rank the performance of algorithms based on the average value, Wilcoxon’s rank test based on median value, and Anova Kruskal–Wallis test are performed. These tests demonstrated the effectiveness of the proposed algorithm.

The proposed QARO is employed to solve a day-ahead EM problem in the MG. A comparison among the convergence characteristics of the proposed QARO algorithm and the original ARO algorithm proves the adequacy of the proposed algorithm in solving the optimization problem. The robustness of the proposed QARO has been validated by comparing its performance on two different MG test systems with other common techniques from the literature (PSO, JAYA, INFO, SO, and the original ARO). The proposed QARO achieved the best solution in the mean, worst, and STD. The total curtailment is 104.97 kWh and 2679.5 MWh in case study 1 and 2, respectively, while the highest benefit is achieved by QARO algorithm is \$50 and \$3010 for the two cases, respectively.

The proposed QARO algorithm can be employed for solving an extended probabilistic energy management problem with considering the uncertainty in the renewable generation, load and energy prices. The Ruidas et al. (2023b) used PSO to optimize the inventory cost related to the investments in reduction of emissions and green innovation. The Quantum behaved PSO (QPSO) is used in Ruidas et al. (2022) to optimize the economic production quantity for production system while in Ruidas et al. (2021) a new inventory cost called development cost is added to the optimization process. Additional QPSO is applied in Ruidas et al. (2023a) to derive the optimal profit in production inventory model for high-tech products. The proposed QARO can be employed to solve these problems and compare its performance with the PSO and QPSO algorithms.

Table 14 Comparison for all studied techniques for case study 2

	PSO	JAYA	INFO	SO	ARO	QARO
Power transaction (MWh)	3453.2	3757.4	3310.2	3264.4	3581.1	3587.4
Total curtailment (MWh)	2193.3	2481.9	24,819	2678.1	2679.4	2679.5
Benefit (\$)	1000	5303	1500.3	1200.1	2000	3010.3

Acknowledgements The icons used through this paper was developed by Freepik, AmethystDesign, Arkinasi and Smashicons from www.flaticon.com.

Funding Open access funding provided by The Science, Technology & Innovation Funding Authority (STDF) in cooperation with The Egyptian Knowledge Bank (EKB). Open access funding provided by The Science, Technology & Innovation Funding Authority (STDF) in cooperation with The Egyptian Knowledge Bank (EKB).

Availability of data and materials Data sharing is not applicable to this article as no datasets were generated or analyses during the current study.

Declarations

Conflict of interest The authors declare that there is no conflict of interest regarding the publication of this manuscript.

Ethical approval This article does not contain any studies with human participants or animals performed by any of the authors.

Informed consent Not applicable.

Open Access This article is licensed under a Creative Commons Attribution 4.0 International License, which permits use, sharing, adaptation, distribution and reproduction in any medium or format, as long as you give appropriate credit to the original author(s) and the source, provide a link to the Creative Commons licence, and indicate if changes were made. The images or other third party material in this article are included in the article's Creative Commons licence, unless indicated otherwise in a credit line to the material. If material is not included in the article's Creative Commons licence and your intended use is not permitted by statutory regulation or exceeds the permitted use, you will need to obtain permission directly from the copyright holder. To view a copy of this licence, visit <http://creativecommons.org/licenses/by/4.0/>.

References

- Aalami HA, Moghaddam MP, Yousefi GR (2010) Demand response modeling considering interruptible/curtailable loads and capacity market programs. *Appl Energy* 87:243–250. <https://doi.org/10.1016/j.apenergy.2009.05.041>
- Aguila-Leon J, Vargas-Salgado C, Chiñas-Palacios C, Díaz-Bello D (2022) Energy management model for a standalone hybrid microgrid through a particle swarm optimization and artificial neural networks approach. *Energy Convers Manag* 267:115920. <https://doi.org/10.1016/j.enconman.2022.115920>
- Ahmadianfar I, Heidari AA, Noshadian S, Chen H, Gandomi AH (2022) INFO: an efficient optimization algorithm based on weighted mean of vectors. *Expert Syst Appl* 195:116516. <https://doi.org/10.1016/j.eswa.2022.116516>
- Alamir N, Kamel S, Megahed TF, Hori M, Abdelkader SM (2022a) Developing an artificial hummingbird algorithm for probabilistic energy management of microgrids considering demand response. *Front Energy Res*. <https://doi.org/10.3389/fenrg.2022.905788>
- Alamir N, Kamel S, Megahed TF, Hori M, Abdelkader SM (2022b) Energy management of microgrid considering demand response using honey badger optimizer. *Renew Energy Power Qual J* 20:12–17. <https://doi.org/10.24084/repqj.20.207>
- Arif A, Javed F, Arshad N (2014) Integrating renewables economic dispatch with demand side management in micro-grids: a genetic algorithm-based approach. *Energy* 7:271–284. <https://doi.org/10.1007/s12053-013-9223-9>
- Biswas PP, Suganthan PN, Mallipeddi R, Amarunga GAJ (2018) Optimal power flow solutions using differential evolution algorithm integrated with effective constraint handling techniques. *Eng Appl Artif Intell* 68:81–100. <https://doi.org/10.1016/j.engappai.2017.10.019>
- Bukar AL, Tan CW, Said DM, Dobi AM, Ayop R, Alsharif A (2022) Energy management strategy and capacity planning of an autonomous microgrid: performance comparison of metaheuristic optimization searching techniques. *Renew Energy Focus* 40:48–66. <https://doi.org/10.1016/j.ref.2021.11.004>
- Coelho LDS (2008) A quantum particle swarm optimizer with chaotic mutation operator. *Chaos Solitons Fractals* 37:1409–1418. <https://doi.org/10.1016/j.chaos.2006.10.028>
- Derrac J, García S, Molina D, Herrera F (2011) A practical tutorial on the use of nonparametric statistical tests as a methodology for comparing evolutionary and swarm intelligence algorithms. *Swarm Evol Comput* 1:3–18
- Dong Y, Liu F, Lu X, Lou Y, Ma Y, Eghbalian N (2022) Multi-objective economic environmental energy management microgrid using hybrid energy storage implementing and developed Manta Ray Foraging Optimization Algorithm. *Electr Power Syst Res* 211:108181. <https://doi.org/10.1016/j.epsr.2022.108181>
- El-Dabah MA, Hassan MH, Kamel S, Abido MA, Zawbaa HM (2023) Optimal tuning of power system stabilizers for a multi-machine power systems using hybrid gorilla troops and gradient-based optimizers. *IEEE Access* 11:27168–27188
- Elkasem AHA, Khamies M, Hassan MH, Agwa AM, Kamel S (2022) Optimal design of TD-TI controller for LFC considering renewables penetration by an improved Chaos game optimizer. *Fractal Fract* 6:220. <https://doi.org/10.3390/fractalfract6040220>
- El-Sattar HA, Kamel S, Hassan MH, Jurado F (2022) Optimal sizing of an off-grid hybrid photovoltaic/biomass gasifier/battery system using a quantum model of Runge Kutta algorithm. *Energy Convers Manag* 258:115539. <https://doi.org/10.1016/j.enconman.2022.115539>
- Fahrioglu M, Alvarado FL (2000) Designing incentive compatible contracts for effective demand management. *IEEE Trans Power Syst* 15:1255–1260. <https://doi.org/10.1109/59.898098>
- Fan Q, Huang H, Li Y, Han Z, Hu Y, Huang D (2021) Beetle antenna strategy based grey wolf optimization. *Expert Syst Appl* 165:113882. <https://doi.org/10.1016/j.eswa.2020.113882>
- Faramarzi A, Heidarinejad M, Stephens B, Mirjalili S (2020) Equilibrium optimizer: a novel optimization algorithm. *Knowl Based Syst* 191:105190. <https://doi.org/10.1016/j.knosys.2019.105190>
- Faria P, Soares J, Vale Z, Morais H, Sousa T (2013) Modified particle swarm optimization applied to integrated demand response and

- DG resources scheduling. *IEEE Trans Smart Grid* 4:606–616. <https://doi.org/10.1109/TSG.2012.2235866>
- Gupta N, Khosravy M, Patel N, Dey N, Mahela OP (2020) Mendelian evolutionary theory optimization algorithm. *Soft Comput* 24:14345–14390
- Hashim FA, Hussien AG (2022) Snake optimizer: a novel meta-heuristic optimization algorithm. *Knowl Based Syst* 242:108320. <https://doi.org/10.1016/j.knosys.2022.108320>
- Jordehi AR (2019) Optimisation of demand response in electric power systems, a review. *Renew Sustain Energy Rev* 103:308–319. <https://doi.org/10.1016/j.rser.2018.12.054>
- Kim H-J, Kim M-K (2019) Multi-objective based optimal energy management of grid-connected microgrid considering advanced demand response. *Energies* 12:4142. <https://doi.org/10.3390/en12214142>
- Lasseter RH (2002) Microgrids. In: *IEEE power engineering society winter meeting. Conference proceedings (Cat. No. 02CH37309), 2002*. IEEE, 305–308. <https://doi.org/10.1109/PESW.2002.985003>
- Mirjalili S, Mirjalili SM, Lewis A (2014) Grey wolf optimizer. *Adv Eng Softw* 69:46–61. <https://doi.org/10.1016/j.advengsoft.2013.12.007>
- Moghaddam AA, Seifi A, Niknam T, Alizadeh Pahlavani MR (2011) Multi-objective operation management of a renewable MG (micro-grid) with back-up micro-turbine/fuel cell/battery hybrid power source. *Energy* 36:6490–6507. <https://doi.org/10.1016/j.energy.2011.09.017>
- Nguyen A-D, Bui V-H, Hussain A, Nguyen D-H, Kim H-M (2018) Impact of demand response programs on optimal operation of multi-microgrid system. *Energies* 11:1452. <https://doi.org/10.3390/en11061452>
- Nwulu NI, Fahrioglu M (2013) A soft computing approach to projecting locational marginal price. *Neural Comput Appl* 22:1115–1124. <https://doi.org/10.1007/s00521-012-0875-8>
- Nwulu NI, Xia X (2017) Optimal dispatch for a microgrid incorporating renewables and demand response. *Renew Energy* 101:16–28. <https://doi.org/10.1016/j.renene.2016.08.026>
- Palensky P, Dietrich D (2011) Demand side management: demand response, intelligent energy systems, and smart loads. *IEEE Trans Ind Inf* 7:381–388. <https://doi.org/10.1109/TII.2011.2158841>
- Parisiso A, Rikos E, Glielmo L (2014) A model predictive control approach to microgrid operation optimization. *IEEE Trans Control Syst Technol* 22:1813–1827. <https://doi.org/10.1109/TCST.2013.2295737>
- Phani-Raghav L, Seshu-Kumar R, Koteswara-Raju D, Singh AR (2022) Analytic hierarchy process (AHP)—swarm intelligence based flexible demand response management of grid-connected microgrid. *Appl Energy* 306:118058. <https://doi.org/10.1016/j.apenergy.2021.118058>
- Rahimiyan M, Baringo L, Conejo AJ (2014) Energy management of a cluster of interconnected price-responsive demands. *IEEE Trans Power Syst* 29:645–655. <https://doi.org/10.1109/TPWRS.2013.2288316>
- Robert FC, Sisodia GS, Gopalan S (2018) A critical review on the utilization of storage and demand response for the implementation of renewable energy microgrids. *Sustain Cities Soc* 40:735–745. <https://doi.org/10.1016/j.scs.2018.04.008>
- Ruidas S, Seikh MR, Nayak PK (2021) A production inventory model with interval-valued carbon emission parameters under price-sensitive demand. *Comput Ind Eng* 154:107154. <https://doi.org/10.1016/j.cie.2021.107154>
- Ruidas S, Seikh MR, Nayak PK (2022) Application of particle swarm optimization technique in an interval-valued EPQ model. In: Anuj K, Sangeeta P, Mangey R, Om Y (eds) *Meta-heuristic optimization techniques*. De Gruyter, Berlin. <https://doi.org/10.1515/9783110716214-004>
- Ruidas S, Seikh MR, Nayak PK (2023a) A production inventory model for high-tech products involving two production runs and a product variation. *J Ind Manag Optim* 19:2178–2205
- Ruidas S, Seikh MR, Nayak PK, Tseng M-L (2023b) An interval-valued green production inventory model under controllable carbon emissions and green subsidy via particle swarm optimization. *Soft Comput*. <https://doi.org/10.1007/s00500-022-07806-1>
- Sedighzadeh M, Esmaili M, Jamshidi A, Ghaderi M-H (2019) Stochastic multi-objective economic-environmental energy and reserve scheduling of microgrids considering battery energy storage system. *Int J Electr Power Energy Syst* 106:1–16. <https://doi.org/10.1016/j.ijepes.2018.09.037>
- Shehzad Hassan MA, Chen M, Lin H, Ahmed MH, Khan MZ, Chughtai GR (2019) Optimization modeling for dynamic price based demand response in microgrids. *J Clean Prod* 222:231–241. <https://doi.org/10.1016/j.jclepro.2019.03.082>
- Shivam R, Dahiya R (2018) Stability analysis of islanded DC microgrid for the proposed distributed control strategy with constant power loads. *Comput Electr Eng* 70:151–162. <https://doi.org/10.1016/j.compeleceng.2018.02.02>
- Soroudi A, Siano P, Keane A (2016) Optimal DR and ESS scheduling for distribution losses payments minimization under electricity price uncertainty. *IEEE Trans Smart Grid* 7:261–272. <https://doi.org/10.1109/TSG.2015.2453017>
- Tazvinga H, Xia X, Zhang J (2013) Minimum cost solution of photovoltaic–diesel–battery hybrid power systems for remote consumers. *Sol Energy* 96:292–299. <https://doi.org/10.1016/j.solener.2013.07.030>
- Tazvinga H, Zhu B, Xia X (2014) Energy dispatch strategy for a photovoltaic–wind–diesel–battery hybrid power system. *Sol Energy* 108:412–420. <https://doi.org/10.1016/j.solener.2014.07.025>
- Torkan R, Ilinca A, Ghorbanzadeh M (2022) A genetic algorithm optimization approach for smart energy management of micro-grid. *Renew Energy* 197:852–863. <https://doi.org/10.1016/j.renene.2022.07.055>
- Wang Y, Huang Y, Wang Y, Zeng M, Li F, Wang Y, Zhang Y (2018) Energy management of smart micro-grid with response loads and distributed generation considering demand response. *J Clean Prod* 197:1069–1083. <https://doi.org/10.1016/j.jclepro.2018.06.271>
- Wang L, Cao Q, Zhang Z, Mirjalili S, Zhao W (2022) Artificial rabbits optimization: a new bio-inspired meta-heuristic algorithm for solving engineering optimization problems. *Eng Appl Artif Intell* 114:105082. <https://doi.org/10.1016/j.engappai.2022.105082>
- Warid W, Hizam H, Mariun N, Abdul-Wahab NI (2016) Optimal power flow using the Jaya algorithm. *Energies* 9:678. <https://doi.org/10.3390/en9090678>
- Wolpert DH, Macready WG (1997) No free lunch theorems for optimization. *IEEE Trans Evol Comput* 1:67–82. <https://doi.org/10.1109/4235.585893>
- Wu X, Zhang S, Xiao W, Yin Y (2019) The exploration/exploitation tradeoff in whale optimization algorithm. *IEEE Access* 7:125919–125928

Yu M, Hong SH (2016) A real-time demand-response algorithm for smart grids: a stackelberg game approach. *IEEE Trans Smart Grid* 7:879–888. <https://doi.org/10.1109/TSG.2015.2413813>

Zhao W, Wang L, Zhang Z (2019) Supply-demand-based optimization: a novel economics-inspired algorithm for global

optimization. *IEEE Access* 7:73182–73206. <https://doi.org/10.1109/ACCESS.2019.2918753>

Publisher's Note Springer Nature remains neutral with regard to jurisdictional claims in published maps and institutional affiliations.